

THE ORDER OF BIFURCATION POINTS IN FOURTH ORDER CONSERVATIVE SYSTEMS VIA BRAIDS

Jan Bouwe van den Berg^{†§}, Miroslav Kramár^{‡¶} and Robert Vandervorst^{†¶}

Abstract. In second order Lagrangian systems bifurcation branches of periodic solutions preserve certain topological invariants. These invariants are based on the observation that periodic orbits of a second order Lagrangian lie on 3-dimensional (non-compact) energy manifolds and the periodic orbits may have various linking and knotting properties. The main ingredients to define the topological invariants are the discretization of second order Lagrangian systems that satisfy the twist property and the theory of discrete braid invariants developed in [4]. In the first part of this paper we recall the essential theory of braid invariants and in the second part this theory is applied to second order Lagrangian system and in particular to the Swift-Hohenberg equation. We show that the invariants yields forcing relations on bifurcation branches. We quantify this principle via an order relation on the topological type of a bifurcation branch. The order will then determine the forcing relation. It is shown that certain braid classes force infinitely many solution curves.

1. Introduction. Fourth order conservative dynamical systems can be viewed as Hamiltonian systems with two degrees of freedom. The dynamics is restricted to 3-dimensional energy surfaces (e.g. [14]) and orbits may display various knotting and linking properties. The knotting information about trajectories provides insight into the dynamics. In particular, forcing solutions based on the existence of other solutions turns out to be a very valuable technique. We divide trajectories into equivalence classes by using the knotting information. Forcing is used to establish a partial order on such classes. In this paper we apply the ideas to the eFK/Swift-Hohenberg equation (see e.g. [8, 2]) and we indicate how these results also apply to fourth order conservative systems in general.

The eFK/Swift-Hohenberg equation is of the form

$$u'''' + \alpha u'' - u + u^3 = 0 \quad \alpha \in \mathbb{R}, \quad (1.1)$$

where $u : \mathbb{R} \rightarrow \mathbb{R}$. When $u(t + \tau) = u(t)$ for some period $\tau > 0$, the solutions are called periodic, or closed characteristics. The equation occurs as the Euler-Lagrange equation of the second order Lagrangian

$$L = \frac{1}{2}|u''|^2 - \frac{\alpha}{2}|u'|^2 + \frac{1}{4}(u^2 - 1)^2,$$

and solutions preserve the energy

$$E = -u'''u' + \frac{1}{2}|u''|^2 - \frac{\alpha}{2}|u'|^2 - \frac{1}{4}(u^2 - 1)^2.$$

[†]Department of Mathematics, VU University Amsterdam, de Boelelaan 1081, 1081 HV Amsterdam, the Netherlands

[‡]Department of mathematics, 110 Frelinghuysen Road, Hill Center Busch Campus, Rutgers University, Piscataway, NJ 08854, USA

[§]J.B. van den Berg was supported by NWO Veni grant 639.031.204.

[¶]M. Kramár and R. Vandervorst were supported by NWO Vidi grant 639.032.202.

The latter defines 3-dimensional (non-compact) energy surfaces M_E that foliate \mathbb{R}^4 . For the values $E = -\frac{1}{4}$ and $E = 0$ the energy surfaces are singular with singularities at $u = 0$ and $u = \pm 1$, respectively.

The level $E = 0$ plays the role of organizing center due to the existence of the equilibrium states $u = \pm 1$. Let us recall the nature of the linearization around the equilibria (see Figure 1.1). The stationary points $u = \pm 1$ change type as function of the parameter α . This happens at the values $\alpha = \pm\sqrt{8}$. For $\alpha \leq -\sqrt{8}$, $u = \pm 1$ are saddles, i.e. real eigenvalues, for $-\sqrt{8} < \alpha < \sqrt{8}$ they are saddle-foci, i.e. complex eigenvalues, and for $\alpha \geq \sqrt{8}$ they are centers, i.e. purely imaginary eigenvalues. For $\alpha \leq -\sqrt{8}$ the set of bounded solutions is very limited. According to [10] the only bounded solutions are the three equilibrium points, two monotone antisymmetric kinks and a one-parameter family of periodic solutions parameterized by the energy E .

At $\alpha = -\sqrt{8}$ an explosion of periodic solutions occurs, see Figure 1.1. Here we restrict attention to the energy level $E = 0$. We classify the periodic solutions as follows. Define the intersection sequence $\sigma = (\sigma_{j_1} \dots \sigma_{j_m})$, $j_k \in \{1, 2\}$, where σ_1 represents the intersections of a periodic function $u(t)$ with $u_- = -1$, while σ_2 represents the intersections with $u_+ = +1$, and all intersections are counted over one period τ . Due to periodicity of u we may assume that σ starts with σ_1 if u intersects u_- . We group the same elements together and use the notation with powers instead of repeating the symbols, e.g. we write $(\sigma_1^2 \sigma_2^2)^2$ instead of $\sigma_1 \sigma_1 \sigma_2 \sigma_2 \sigma_1 \sigma_1 \sigma_2 \sigma_2$. The number of crossings of a periodic solution u with u_{\pm} is the number of zeros of the functions $u - u_{\pm}$ counted over the period without multiplicity, i.e., every zero is counted just once even if it is a multiple zero. The zero points are isolated and this number is well defined and finite and preserved along the continuous bifurcation branches, see [8]. We distinguish different classes of periodic functions based on their intersections σ .

Definition 1.1. *Periodic functions u are categorized by the following three classes:*

- (I) $\sigma = (\sigma_1^2 \sigma_2^2)^q$, for some $q \in \mathbb{N}$;
- (II) both σ_1 and σ_2 are present in σ , but $\sigma \neq (\sigma_1^2 \sigma_2^2)^q$ for any $q \in \mathbb{N}$;
- (III) $\sigma = (\sigma_1^{2q})$, or $\sigma = (\sigma_2^{2q})$, for some $q \in \mathbb{N}$.

The sequence σ will be called the intersection sequence of u .

Further classification can be carried out by counting the monotone laps of a periodic solution. It was shown in [14] that if a second order Lagrangian system satisfies a twist property (see Section 2), then every solution is a concatenation of regular monotone laps between extrema and degenerate monotone laps, and the number of all monotone laps is finite and even per period. A regular monotone lap is a segment of the solution u such that u' does not change sign, i.e. $u' < 0$ or $u' > 0$, and a degenerate monotone lap is an inflection point. We have to count both non-degenerate and degenerate monotone laps in order to obtain the invariant along the bifurcation branch. The same type of arguments that are used to show that the number of crossings with u_{\pm} is preserved along the solution branch imply that a regular monotone lap can disappear only by becoming a degenerate monotone lap, see again [8].

Definition 1.2. *Let u be a periodic solution of Equation (1.1) at the energy level $E = 0$, with intersection sequence σ and $2p$ monotone laps per period, then u is said to be of the type $[\sigma, p]$.*

Question: Does there exist a periodic solution u on $E = 0$ for any given type $[\sigma, p]$?

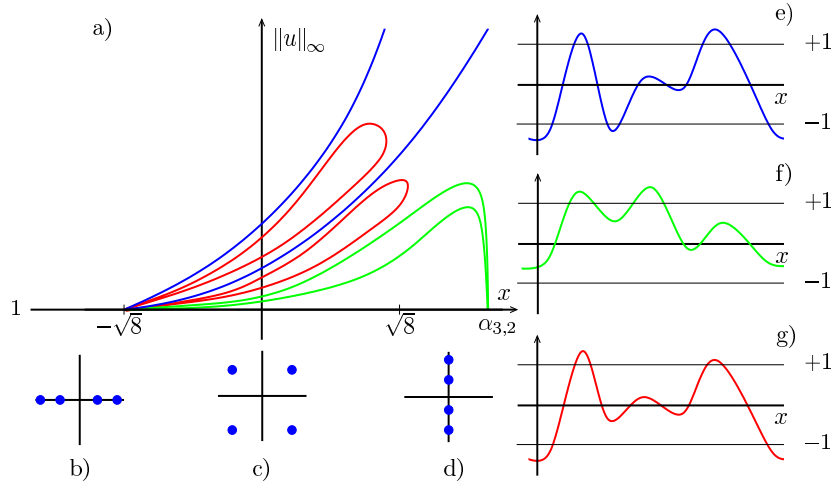


Figure 1.1. Bifurcation diagram (a) shows three different classes of branches, which bifurcate from $u = -1$ at $\alpha = -\sqrt{8}$. Solutions on the branches that extend beyond the boundary of the diagram are of the first class (see (e)), branches that form closed loops consist of solutions of the second class (see (f)), and branches collapsing onto $u = -1$ consist of solutions of the third class (see (g)). Also depicted are the spectra of the linearization around $u = +1$ and $u = -1$, see (b) for $\alpha \leq -\sqrt{8}$, (c) for $\alpha \in (-\sqrt{8}, \sqrt{8})$, and (d) for $\sqrt{8} \leq \alpha$.

We stress that the type $[\sigma, p]$ is an invariant in the sense that it is conserved along continuous branches of solutions (in $E = 0$) when varying the parameter α . As it turns out, most of the interesting behaviour occurs when the equilibria $u = \pm 1$ are saddle-foci, i.e. $\alpha \in (-\sqrt{8}, \sqrt{8})$. The saddle-focus behaviour near $u = \pm 1$ allows us to control the flow near the equilibria, which are singular points in the energy manifold. For technical reasons we will in this paper consider the parameter range $\alpha \in [0, \sqrt{8})$ only. However the machinery developed in this paper can be readily applied to the positive energy levels for $\alpha \geq \sqrt{8}$ where the constant solutions $u_\pm = \pm 1$ are replaced by the small oscillations constructed in [12]. The limit process used in [12] may be used to further extend our result for $\alpha \geq \sqrt{8}$. For a wealth of results about periodic solutions in the parameter range $\alpha \in (-\sqrt{8}, 0)$ we refer to [6].

For periodic functions of class (I) and (III), see Definition 1.1, the pair (p, q) determines the type $[\sigma, p]$. For class (II) this obviously does not hold. In [4] it is proved that for the entire parameter range $\alpha \geq 0$, there exists at least one periodic solution of class (I) for any coprime pair (p, q) ¹, see also Figure 1.1(a,e). In [12] the case of periodic solutions of class (III) is treated and it is shown that for $0 \leq \alpha < \alpha_{p,q} := \sqrt{2} \left(\frac{p}{q} + \frac{q}{p} \right)$ there is at least one periodic solution of class (III) at the energy surface $E = 0$, for any coprime pair (p, q) . As illustrated in Figure 1.1(a,f) these solutions converge to one of the equilibria $u = \pm 1$ as α tends to $\alpha_{p,q}$.

For class (I) and class (III) the above question has thus been addressed in [4] and [12]. In order to deal with class (II) solutions, the subject of this paper, yet another structure is needed. We refine the existence question to a forcing problem: for arbitrary $\alpha \in [0, \sqrt{8})$, given a periodic solution of type $[\sigma, p]$, does this force the existence of a periodic solution of type $[\sigma', p']$? We will

¹The existence actually extends to $\alpha > -\sqrt{8}$, see [9].

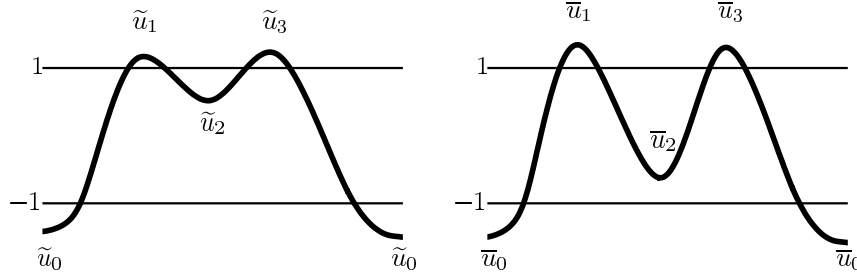


Figure 1.2. Sketch of two periodic solutions $\tilde{u}, \bar{u} \in [\sigma_1^2 \sigma_2^4, 2]$. Their extrema points are labeled by \tilde{u}_i and \bar{u}_i . The most obvious difference between the solutions \tilde{u} and \bar{u} is the position of the extremal points \tilde{u}_2 and \bar{u}_2 .

think of forcing in terms of a partial order on the types $[\sigma, p]$. To be more precise, if a periodic solution of type $[\sigma, p]$ of (1.1) for some $\alpha \in [0, \sqrt{8})$ forces the existence of a periodic solution of type $[\sigma', p']$ of (1.1) for the same value of α , then $[\sigma, p]$ is said to precede $[\sigma', p']$. Notation:

$$[\sigma, p] \prec [\sigma', p'].$$

Clearly, this definition means very little for types $[\sigma, p]$ corresponding to class (I) and class (III), since they are known to exist for all $\alpha \leq \alpha_{p,q} \geq \sqrt{8}$, respectively. On the other hand, for class (II) solutions unravelling the partial ordering is a challenge. The ordering has important implications for the bifurcation diagram of Equation (1.1). If Γ and Γ' are continuous curves corresponding to solutions of the class $[\sigma, p]$ and $[\sigma', p']$ respectively, and $[\sigma, p] \prec [\sigma', p']$, then Γ' has to exist at least as long as Γ does. In other words, in Figure 1.1(a) the saddle-node bifurcation for Γ occurs at a smaller value of α than the one for Γ' .

The intricate ordering of such saddle-node bifurcations was first studied for homoclinic solutions of a slight variation of Equation (1.1) in [1], where a list of rules was proposed based on the folding of the stable and unstable manifolds. Our approach here is entirely different, based on topological properties of the solutions, and we rigorously determine an important part of this ordering from which many existence result can be extracted.

Before stating the main result we start with an important example.

Example 1.3. For Equation (1.1) the existence of a solution $\tilde{u} \in [\sigma_1^2 \sigma_2^4, 2]$ is shown in [6] for $\alpha \in [-\sqrt{8}, \varepsilon]$, where $\varepsilon > 0$ is sufficiently small. This solution is a minimizer of the underlying Lagrangian system, and hence its Morse index is zero. Its extremal points $\tilde{u}_1, \tilde{u}_2, \tilde{u}_3$ are very close to $u_+ = 1$, see Figure 1.2(a). Numerics suggest that there is another solution with the Morse index one in the same class. This solution has a slightly different shape (see Figure 1.2(b)), the local minimum \bar{u}_2 being near -1 . The type $[\sigma, p]$ represents a class of periodic functions to which we will assign a topological invariant. For this invariant the Morse relations apply, see Section 3. The invariant of $[\sigma_1^2 \sigma_2^4, 2]$ is trivial, which implies that the solution \tilde{u} cannot be the only one in this class. Numerics suggest that these two solutions are on the same bifurcation branch which forms a loop, see Figure 1.1. The loop turns at some point $\alpha^* > 0$, where these two solutions coalesce (saddle-node). Rigorous numerics is used in [13] to prove the existence of a solution $\tilde{u} \in [\sigma_1^2 \sigma_2^4, 2]$ for $\alpha \in [0, \alpha^*]$, where $\alpha^* > 2$ (in fact $\alpha^* \approx 2.03$, see [11]). Any type of solution forced by $[\sigma_1^2 \sigma_2^4, 2]$ (i.e. preceded by it in the ordering) thus also exists for $\alpha \in [0, \alpha^*]$ at the least.

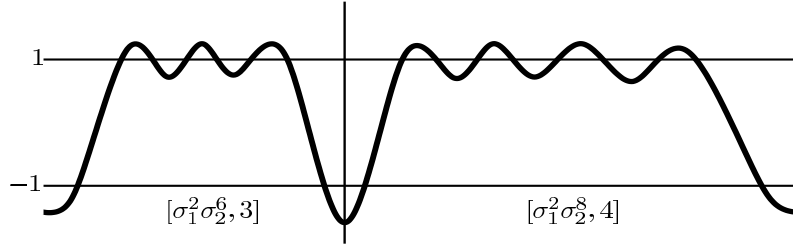


Figure 1.3. Sketch of a periodic solution $u \in [\sigma_1^2 \sigma_2^6 \sigma_1^2 \sigma_2^8, 7]$ which consists of two blocks, namely $[\sigma_1^2 \sigma_2^6, 3]$ and $[\sigma_1^2 \sigma_2^8, 4]$.

In the same paper the existence of a multitude of solutions is proved using a forcing relation. In Figure 1.3 the types of solutions are indicated. We translate this statement, proved in [13], to the context of the present paper in the following proposition.

Proposition 1.4. Let $\alpha \in [0, \sqrt{8})$ and $q_1, \dots, q_n \in \mathbb{N}$ with $q_i > 1$. Then

$$[\sigma_1^2 \sigma_2^4, 2] \prec [\sigma_1^2 \sigma_2^{2q_1} \dots \sigma_1^2 \sigma_2^{2q_n}, p],$$

where $p = \sum_{i=1}^n q_i$.

The idea behind Proposition 1.4 is concatenation of types based on the forcing relation $[\sigma_1^2 \sigma_2^4, 2] \prec [\sigma_1^2 \sigma_2^{2p}, p]$. The set of types

$$\mathcal{Z} = \left\{ [\sigma, p] \mid \sigma = \sigma_1^2 \sigma_2^{2q_1} \dots \sigma_1^2 \sigma_2^{2q_n}, \sum_i q_i \leq p \right\},$$

can be given a semi-group structure as follows: $[\sigma, p] \cdot [\sigma', p'] := [\sigma \sigma', p + p']$. This multiplication make (\mathcal{Z}, \cdot) a non-commutative semi-group. We can introduce a unit element in \mathcal{Z} by allowing constant solutions. This then gives (\mathcal{Z}, \cdot) the structure of a monoid. Elements of the form $[\sigma_1^2 \sigma_2^{2q}, p]$, called *fundamental blocks*, serve as generators of \mathcal{Z} and particular $[\sigma_1^2 \sigma_2^{2q_1} \dots \sigma_1^2 \sigma_2^{2q_n}, p] = \prod_i [\sigma_1^2 \sigma_2^{2q_i}, p_i]$, where $p = \sum_i p_i$, i.e., any type in \mathcal{Z} can be represented as a product of fundamental blocks. Note that this representation is not unique in general. Uniqueness holds if $q_i = p_i$ for all i . With respect to ordering and multiplication the following result holds.

Theorem 1.5. If Proposition 1.4 and Theorem 1.6 imply that $[\sigma_1^2 \sigma_2^4, 2]$ predeces two types $[\sigma, p], [\sigma', p'] \in \mathcal{Z}$, then

$$[\sigma_1^2 \sigma_2^4, 2] \prec [\sigma, p] \cdot [\sigma', p'],$$

with $[\sigma, p] \cdot [\sigma', p'] := [\sigma \sigma', p + p']$. Since it was proved in [13] that $[\sigma_1^2 \sigma_2^4, 2] \prec [\sigma_1^2 \sigma_2^{2p}, p]$ (i.e. $q = p$), Proposition 1.4 follows from Theorem 1.5 by considering types $[\sigma_1^2 \sigma_2^{2q_i}, q_i]$ and taking products. In this paper we extend the result in [13] to types of the form $[\sigma_1^2 \sigma_2^{2q_1} \dots \sigma_1^2 \sigma_2^{2q_n}, p]$, with $p \leq \sum_{i=1}^n q_i$. The crucial element is to establish the ordering for types $[\sigma_1^2 \sigma_2^{2q}, p]$, $q \leq p$ and build the more complicated types by concatenating the fundamental blocks using Theorem 1.5.

Theorem 1.6. Let $\alpha \in [0, \sqrt{8})$ and $p, q \in \mathbb{N}$ such that $3 < q < p$. Then,

$$[\sigma_1^2 \sigma_2^4, 2] \prec [\sigma_1^2 \sigma_2^{2q}, p],$$

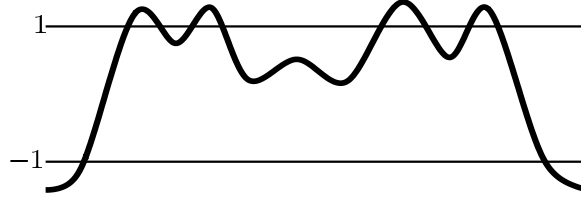


Figure 1.4. Sketch of a periodic solution $u \in [\sigma_1^2 \sigma_2^8, 5]$.

which extends the case $p = q$ (Proposition 1.4). Theorem 1.6 is ultimately at the heart of the matter and its proof involves a very intricate induction argument on p (for fixed q), exploiting Mayer-Vietoris sequences in homology, see Section 6.4.

An example of a solution of the class $[\sigma_1^2 \sigma_2^8, 5]$ is depicted in Figure 1.4. Now consider types of the form $[\sigma_1^2 \sigma_2^{2q_1} \dots \sigma_1^2 \sigma_2^{2q_n}, p]$, with $q_i > 1$ and $\sum_{i=1}^n q_i \leq p$. The case $\sum_{i=1}^n q_i = p$ is covered by Proposition 1.4. For the general case $\sum_{i=1}^n q_i \leq p$ we have:

Theorem 1.7. *Let $\alpha \in [0, \sqrt{8}]$. For any representation $[\sigma_1^2 \sigma_2^{2q_1} \dots \sigma_1^2 \sigma_2^{2q_n}, p] = \prod_i [\sigma_1^2 \sigma_2^{2q_i}, p_i]$, with either $3 < q_i < p$, or $2 \leq q_i = p_i$, it holds that*

$$[\sigma_1^2 \sigma_2^4, 2] \prec [\sigma_1^2 \sigma_2^{2q_1} \dots \sigma_1^2 \sigma_2^{2q_n}, p],$$

where $p = \sum_{i=1}^n p_i$.

The forcing relations of Proposition 1.4 and Theorem 1.7 imply the existence of many solutions and indicate that all forced types have turning points at values of α larger than α^* (the saddle-node bifurcation for the type $[\sigma_1^2 \sigma_2^4, 2]$). Additionally, instead of finding just one solution of the class $[\sigma_1^2 \sigma_2^{2q_1} \dots \sigma_1^2 \sigma_2^{2q_n}, p]$, the forcing relation yields a lower bound on the number of solutions that are forced based on the topological data of the type $[\sigma, p]$. Different solutions $u \in [\sigma, p]$ may braid around the solution \tilde{u} in topologically different ways. The following theorems estimate the number of geometrically different solutions within the classes $[\sigma_1^2 \sigma_2^{2q}, p]$ and $[\sigma_1^2 \sigma_2^{2q_1} \dots \sigma_1^2 \sigma_2^{2q_n}, p]$. For counting purposes we introduce

$$\beta_{q,p} = \begin{cases} 1 & \text{for } q = p = 2, \\ 2^{p-3} & \text{for } q = p \geq 3, \\ 1 & \text{for } 4 = q < p, \\ 2^{q-5} & \text{for } 5 \leq q < p. \end{cases}$$

Theorem 1.8. *Let $\alpha \in [0, \alpha^*]$ and $p \in \mathbb{N}$ such that $p \geq 2$. Then there are at least $\beta_{p,p}$ geometrically distinct solutions of the solution class $[\sigma_1^2 \sigma_2^{2p}, p]$. If $q \in \mathbb{N}$ is such that $3 < q < p$, then there are at least $\beta_{p,q}$ geometrically distinct solutions of the class $[\sigma_1^2 \sigma_2^{2q}, p]$. Figure 1.5 shows the different geometries of the solutions of type $[\sigma_1^2 \sigma_2^{2p}, p]$ and the combinatorics of counting different solutions by considering patterns with ‘fingers’. The part of Theorem 1.8 that*

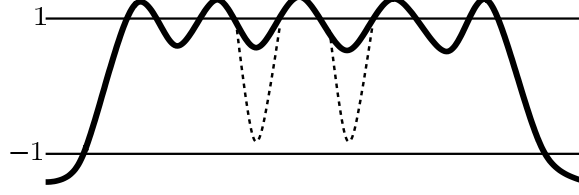


Figure 1.5. For the type $[\sigma_1^2 \sigma_2^{10}, 5]$ either zero, one, or two fingers can be considered in a total of four configurations between the first and last oscillation around $u = +1$.

deals with solutions in the class $[\sigma_1^2 \sigma_2^{2p}, p]$ is proved in Section 6, while the rest of the proof is carried out in the last section. Theorem 1.8 can be used to give a lower bound on the number of solutions in $[\sigma_1^2 \sigma_2^{2q_1} \dots \sigma_1^2 \sigma_2^{2q_n}, p]$.

Theorem 1.9. Let $\alpha \in [0, \alpha^*]$. For the types $[\sigma_1^2 \sigma_2^{2q_1} \dots \sigma_1^2 \sigma_2^{2q_n}, p] = \prod_i [\sigma_1^2 \sigma_2^{2q_i}, p_i]$ as described in Theorem 1.7 the lower bound on the number of solutions is given by $\prod_i \beta_{p_i, q_i}$.

The above theorems are established via a Morse type theory using Conley index and braid theory, see [4]. As a by-product we obtain estimates on the Morse indices $\mu(u)$ of solutions u . For example, for solutions with fingers, as depicted in Figure 1.5, the number of fingers determine the Morse index. To be more precise, for the case $q_i = p_i$, generically

$$\mu(u) = \# \text{ fingers.}$$

For other type of solutions we obtain similar relations, and we refer the reader to the forthcoming sections.

Remark 1.10. In this paper we restricted the forcing relations to the ‘base’ type $[\sigma_1^2 \sigma_2^4, 2]$. The exact same results follows for the base type $[\sigma_1^4 \sigma_2^2, 2]$. The results even extend if we consider the base type $[\sigma_1^4 \sigma_2^4, 3]$. In this case we obtain fingers towards both $u = +1$ and $u = -1$. The results are not restricted to the specific Equation (1.1) but apply to any second order Lagrangian twist system with at least two equipotential states. Clearly, the analysis in this paper only reveals a small portion of the partial order on types. The techniques described in this paper can also be used to further study the partial order relation for other types, the type $[\sigma_1 \sigma_2^6, 3]$ begin the first obvious candidate.

2. Reduction to a finite dimensional problem. In this section we give a brief survey of the reduction of the problem of finding periodic solutions for Equation (1.1) to the problem of finding fixed points of a vector field generated by a parabolic recurrence relation. We present this approach in the context of general second order Lagrangians.

If we seek closed characteristics i.e., periodic solutions of Equation (1.1) at a given energy level E we can invoke the following variational principle:

$$\text{Extremize } \{J_E[u] : u \in \Omega_{\text{per}}, \tau > 0\}, \quad (2.1)$$

where $\Omega_{\text{per}} = \cup_{\tau > 0} C^2(S^1, \tau)$, the periodic functions with period τ , and

$$J_E[u] = \int_0^\tau (L(u, u', u'') + E) dt. \quad (2.2)$$

The function $L \in C^2(\mathbb{R}^3, \mathbb{R})$ is assumed to satisfy $\frac{\partial^2 L}{\partial w^2}(u, v, w) \geq \delta > 0$ for all $(u, v, w) \in \mathbb{R}^3$. For the general second order Lagrangian system the (conserved) energy is given by

$$\mathbb{E}[u] = \left(\frac{\partial L}{\partial u'} - \frac{d}{dt} \frac{\partial L}{\partial u''} \right) u' + \frac{\partial L}{\partial u''} u'' - L(u, u', u''). \quad (2.3)$$

It follows from [14] that the variations in τ guarantee that any critical point u of (2.1) has energy $\mathbb{E}[u] = E$. An energy value E is called regular if $\frac{\partial L}{\partial u}(u, 0, 0) \neq 0$ for all u that satisfy $L(u, 0, 0) + E = 0$. The energy manifold $M_E \subset \mathbb{R}^4$ for a regular energy value E is a smooth non-compact manifold without boundary. For a fixed regular energy value E , the extrema of a closed characteristic are contained in the closed set $\{u : L(u, 0, 0) + E \geq 0\}$. The connected components I_E of this set are called *interval components*. Moreover, it follows from [14] that solutions on a regular energy level do not have inflection points. For a singular energy level the interval component I_E contains critical points and the situation is more complicated.

It was shown in [14] that for Lagrangian systems $J[u] = \int_I L(u, u', u'') dt$ with $L(u, u', u'') = \frac{1}{2}u''^2 + K(u, u')$, at energy levels E which satisfy

$$\frac{\partial K}{\partial v} v - K(u, v) - E \leq 0 \text{ for all } u \in I_E \text{ and } v \in \mathbb{R}, \quad (2.4a)$$

$$\frac{\partial^2 K}{\partial v^2} v^2 - \frac{5}{2} \left\{ \frac{\partial K}{\partial v} - K(u, v) - E \right\} \geq 0 \text{ for all } u \in I_E \text{ and } v \in \mathbb{R}, \quad (2.4b)$$

there is a unique pair (τ, u_τ) minimizing

$$\inf_{u \in X_\tau, \tau \in \mathbb{R}^+} \int_0^\tau (L(u, u', u'') + E) dt,$$

with $X_\tau(u_1, u_2) = \{u \in C^2([0, \tau]) : u(0) = u_1, u(\tau) = u_2, u'(0) = u'(\tau) = 0, u'|_{(0, \tau)} > 0 \text{ if } u_1 < u_2 \text{ and } u'|_{(0, \tau)} < 0 \text{ if } u_1 > u_2\}$ for $(u_1, u_2) \in I_E \times I_E \setminus \Delta$ and $\Delta = \{(u_1, u_2) \in I_E \times I_E : u_1 = u_2\}$. Moreover, the function defined by

$$S_E(u_1, u_2) = \inf_{u \in X_\tau, \tau \in \mathbb{R}^+} \int_0^\tau (L(u, u', u'') + E) dt, \quad (2.5)$$

for $(u_1, u_2) \in I_E \times I_E \setminus \Delta$, and $S_E|_\Delta = 0$, has the following properties (see[14]):

- (a) $S_E \in C^2(I_E \times I_E \setminus \Delta)$.
- (b) $\partial_1 \partial_2 S_E(u_1, u_2) > 0$ for all $u_1 \neq u_2 \in I_E$.
- (c) $\lim_{u_1 \nearrow u_2} -\partial_1 S_E(u_1, u_2) = \lim_{u_2 \searrow u_1} \partial_2 S_E(u_1, u_2) =$
 $= \lim_{u_1 \searrow u_2} \partial_1 S_E(u_1, u_2) = \lim_{u_2 \nearrow u_1} -\partial_2 S_E(u_1, u_2) = +\infty$.

The function S_E is a *generating function* and a Lagrangian system possessing such a generating function is called a *twist system*. The second order Lagrangian system associated to Equation (1.1) is a twist system for $\alpha \geq 0$. For more examples see [14].

The question of finding closed characteristics for a twist system can now be formulated in terms of S_E . Any periodic solution u is a concatenation of monotone laps. Let us take an arbitrary $2p$ periodic sequence $\{u_i\}$ and define u as a concatenation of monotone laps (minimizers

$u_\tau(u_i, u_{i+1})$) between the consecutive extremal points u_i solving the Euler-Lagrange equation in between any two extrema. The concatenation u does not have to be a solution on \mathbb{R} because the third derivatives of two monotone laps do not have to match at the extremal point u_i . It was proved in [14] that the third derivatives match if and only if the extrema sequence $\{u_i\}$ is a critical point of discrete action

$$W_{2p} = \sum_{i=0}^{2p-1} S_E(u_i, u_{i+1}). \quad (2.6)$$

Critical points of W_{2p} satisfy equations

$$\mathcal{R}_i(u_{i-1}, u_i, u_{i+1}) = \partial_2 S_E(u_{i-1}, u_i) + \partial_1 S_E(u_i, u_{i+1}) = 0, \quad (2.7)$$

where $\mathcal{R}_i(s, t, r)$ is, according to property (a), well-defined and C^1 on the following domains

$$\Omega_i = \{(r, s, t) \in I_E^3 : (-1)^{i+1}(s-r) > 0, (-1)^{i+1}(s-t) > 0\}. \quad (2.8)$$

The functions \mathcal{R}_i and domains Ω_i satisfy $\mathcal{R}_i = \mathcal{R}_{i+2}$ and $\Omega_i = \Omega_{i+2}$ for $i \in \mathbb{Z}$ (alternating increasing and decreasing laps). Property (b) implies that $\partial_1 \mathcal{R}_i = \partial_1 \partial_2 S(u_{i-1}, u_i) > 0$, and $\partial_3 \mathcal{R}_i = \partial_1 \partial_2 S(u_i, u_{i+1}) > 0$. Property (c) provides information about the behavior of \mathcal{R}_i at the diagonal boundaries of Ω_i , namely,

$$\lim_{s \searrow r} \mathcal{R}_i(r, s, t) = \lim_{s \searrow t} \mathcal{R}_i(r, s, t) = +\infty, \quad (2.9)$$

$$\lim_{s \nearrow r} \mathcal{R}_i(r, s, t) = \lim_{s \nearrow t} \mathcal{R}_i(r, s, t) = -\infty. \quad (2.10)$$

Above-mentioned properties of \mathcal{R}_i give us that \mathcal{R}_i is parabolic recurrence relation of up-down type as defined below. First, we define parabolic recurrence relations.

Definition 2.1. A parabolic recurrence relation \mathcal{R} on $\mathbb{R}^{\mathbb{Z}}$ is a sequence of real-valued functions $\mathcal{R} = (\mathcal{R}_i)_{i \in \mathbb{Z}}$ satisfying

(A1): [monotonicity] $\partial_1 \mathcal{R}_i > 0$ and $\partial_3 \mathcal{R}_i > 0$ for all $i \in \mathbb{Z}$

(A2): [periodicity] for some $d \in \mathbb{N}$, $\mathcal{R}_{i+d} = \mathcal{R}_i$ for all $i \in \mathbb{Z}$.

We see that our \mathcal{R} is not a parabolic recurrence relation in the strict sense because it is not defined on whole space $\mathbb{R}^{\mathbb{Z}}$. It is not defined for any sequence satisfying $u_i = u_{i+1}$ for some $i \in \mathbb{Z}$. This corresponds to the nature of solutions of Equation (1.1), namely that minima and maxima alternate.

Definition 2.2. A parabolic recurrence relation \mathcal{R} defined on domain given by (2.8) is said to be of up-down type if (2.9) and (2.10) are satisfied.

These results can be summarized in terms of parabolic recurrence relation as follows.

Proposition 2.3. Let $J[u] = \int L(u, u', u'') dt$ be a second order Lagrangian twist system. Suppose that W_{2p} is the discrete action defined through (2.5) and (2.6) at the regular energy level E . Then

- (a) the functions $\mathcal{R}_i = \partial_i W_{2p}$ defined on Ω_i are components of a parabolic recurrence relation \mathcal{R} of up-down type,
- (b) solutions of $\mathcal{R} = 0$ correspond to periodic solutions on the energy level E .

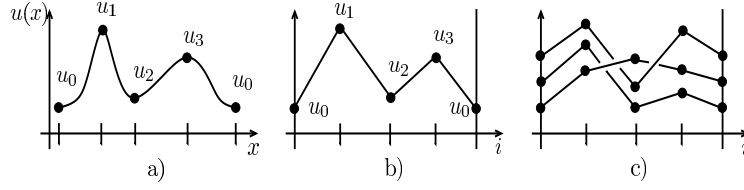


Figure 2.1. (a) A periodic function and (b) its piecewise linear graph (c) a braid consisting of 3 strands.

The parabolic recurrence relation is both exact and up-down type. In order to find solutions of $\mathcal{R} = 0$ we will employ the Conley index. Conley index theory gives information about the invariant set of a flow inside an isolating neighborhood for this flow. In the case of a gradient vector field invariant sets have special structure and thus information about critical points can be obtained. There is a natural way to define a flow generated by an up-down parabolic recurrence relation on the set

$$\Omega^{2p} = \{\mathbf{u} \in \mathbb{R}^{\mathbb{Z}} : \mathbf{u} \text{ is } 2p \text{ periodic and } (u_{i-1}, u_i, u_{i+1}) \in \Omega^i, \text{ for } i \in \mathbb{Z}\}. \quad (2.11)$$

Consider the differential equations

$$\frac{d}{dt} u_i(t) = \mathcal{R}_i(\mathbf{u}(t)), \quad \mathbf{u}(t) \in \Omega^{2p}, \quad t \in \mathbb{R}. \quad (2.12)$$

Equation (2.12) defines a (local) C^1 flow ψ^t on Ω^{2p} . This flow is not defined at the boundary of Ω^{2p} , but conditions (2.9) and (2.10) give us information about the flow close to this boundary. Finding a periodic solution within the class $[\sigma, p]$ can be reduced to constructing an appropriate isolating neighborhood for the flow ψ^t and calculating its (nontrivial) Conley index. We will use the concept of up-down discretized braid diagrams to construct this isolating neighborhood. For any $2p$ -periodic extrema sequence we can construct a piecewise linear graph by connecting the consecutive points $(i, u_i) \in \mathbb{R}^2$ by straight line segments. The piecewise linear graph, called a strand, is cyclic: one restricts to $0 \leq i \leq 2p$ and identifies the end points abstractly. A collection of n closed characteristics of period $2p$ then gives rise to a collection of n strands. For multiple strands we can replace the periodicity of a single sequence to a braid structure by matching the beginning and end points and assigning a crossing type (positive) to every transverse intersection of the graphs: larger slope crosses over smaller slope, see Figure 2.1. We represent sequences of extrema in the space of closed, positive, piecewise linear braid diagrams. We briefly recall some basic facts from (discrete) braid theory (for more details see [4]).

3. Braid invariants and the Conley Index. We recall now the basic theory of proper braid classes and the Conley type braid invariants, and the implications for parabolic recurrence relations [4]. The parabolic recurrence relations coming from fourth order conservative systems, as explained in the previous section, can be put into this framework.

3.1. Braid invariants. **Definition 3.1.** Denote by \mathcal{D}_d^n the space of all closed piecewise linear braid diagrams (PL-braid diagrams) on n strands with period d . That is, the space of all (unordered) collections $\beta = \{\beta^k\}_{k=1}^n$ of continuous maps $\beta^k : [0, 1] \rightarrow \mathbb{R}$ such that

- (a) β^k is affine linear on $[\frac{i}{d}, \frac{i+1}{d}]$ for all k and for all $i = 0, \dots, d-1$;
 (b) $\beta^k(0) = \beta^{\tau(k)}(1)$ for some permutation τ ;
 (c) for any s such that $\beta^k(s) = \beta^l(s)$ with $k \neq l$, the crossing is transversal: for ϵ sufficiently small

$$(\beta^k(s - \epsilon) - \beta^l(s - \epsilon))(\beta^k(s + \epsilon) - \beta^l(s + \epsilon)) < 0.$$

Any PL-braid diagram corresponds to some n -collection $\mathbf{u} = \{\mathbf{u}^k\}_{k=0}^{n-1}$ of anchor points $\mathbf{u}^k = \{u_i^k\}$, where

$$u_i^k = \beta^k(i/d), \quad (3.1)$$

The converse to this statement is not true because condition (c) of Definition 3.1 is not satisfied for arbitrary collection of sequences. A collection \mathbf{u} for which this condition is violated corresponds to a singular PL-braid diagram. We switch between the notation u_i^k of the anchor points and β^k of the piecewise linear braid diagrams throughout this section, using β only if necessary. Discretized braid diagrams will primarily be denoted by \mathbf{u} . Given anchor points \mathbf{u} , the associated piece wise linear braid diagram is given by $\beta(\mathbf{u})$.

Two representatives $\mathbf{u}, \mathbf{u}' \in \mathcal{D}_d^n$ are of the same discretized braid class $[\mathbf{u}] = [\mathbf{u}']$, if and only if they are in the same connected component of \mathcal{D}_d^n . Note that if $[\mathbf{u}] = [\mathbf{u}']$, then $\beta(\mathbf{u})$ and $\beta(\mathbf{u}')$ are isotopic as closed positive topological braid diagrams (and braids), see [4]. However, two discretizations of a topological braid are not necessarily equivalent in \mathcal{D}_d^n , i.e. connected in \mathcal{D}_d^n . The connected component $[\mathbf{u}]$ of \mathcal{D}_d^n are called *braid classes* of period d . The singular braids \mathbf{u} are defined by $\Sigma_d^n := \overline{\mathcal{D}_d^n} \setminus \mathcal{D}_d^n$ and consists of braids \mathbf{u} failing (c) in Definition 3.1. We suppress the indices and denote the semi-algebraic sub-variety of singular braids by Σ . The set $\Sigma_- \subset \Sigma$ denotes the collapsed singularities; roughly speaking, in Σ_- some of the strands coincide completely (at all anchor points), see [4] for details.

For pairs of braids we can define the space of braid pairs using the fact that the union of two braid diagrams is again a braid diagram satisfying (a) and (b) of Definition 3.1. Consider

$$\mathcal{D}_d^{n,m} := \{(\mathbf{u}, \mathbf{v}) \in \mathcal{D}_d^n \times \mathcal{D}_d^m \mid \mathbf{u} \cup \mathbf{v} \in \mathcal{D}_d^{n+m}\}. \quad (3.2)$$

For pairs $(\mathbf{u}, \mathbf{v}) \in \mathcal{D}_d^{n,m}$ we write $\mathbf{u} \# \mathbf{v}$. Note that for $\mathbf{u} \# \mathbf{v} \in \mathcal{D}_d^{n,m}$ it holds $\mathbf{u} \in \mathcal{D}_d^n$ and $\mathbf{v} \in \mathcal{D}_d^m$. As before the connected components of $\mathcal{D}_d^{n,m}$ are denoted by $[\mathbf{u} \# \mathbf{v}]$ and are called *relative braid classes* (of period d). Associated with $[\mathbf{u} \# \mathbf{v}]$ we have the projection

$$\pi : \mathcal{D}_d^{n,m} \rightarrow \mathcal{D}_d^m, \quad \mathbf{u} \# \mathbf{v} \mapsto \mathbf{v}.$$

For each $\mathbf{v}' \in \pi([\mathbf{u} \# \mathbf{v}])$ we can define the fiber $[\mathbf{u}'] \text{ rel } \mathbf{v}' := \{\mathbf{u}' \in \mathcal{D}_d^n \mid \mathbf{u}' \# \mathbf{v}' \in [\mathbf{u} \# \mathbf{v}]\}$. The fiber $[\mathbf{u}'] \text{ rel } \mathbf{v}'$ is called a *relative braid class with fixed skeleton* \mathbf{v}' . Depending on the period d a fiber $[\mathbf{u}'] \text{ rel } \mathbf{v}'$ may consists of more than one connected component. The set of connected components relative to a fixed braid $\mathbf{v} \in \mathcal{D}_d^m$ is denoted by $\mathcal{D}_d^n \text{ rel } \mathbf{v}$.

Definition 3.2. A relative braid class $[\mathbf{u} \# \mathbf{v}] \subset \mathcal{D}_d^{n,m}$ is called *bounded* if every fiber $[\mathbf{u}'] \text{ rel } \mathbf{v}'$ with $\mathbf{v}' \in \pi([\mathbf{u} \# \mathbf{v}])$, is a bounded set.

As before we can define the singular relative braids as $\Sigma_d^n \text{ rel } \mathbf{v} := \overline{\mathcal{D}_d^n} \text{ rel } \mathbf{v} \setminus \mathcal{D}_d^n \text{ rel } \mathbf{v}$ and $\Sigma_- \text{ rel } \mathbf{v} := \Sigma_-^{n+m} \cap (\overline{\mathcal{D}_d^n} \text{ rel } \mathbf{v})$.

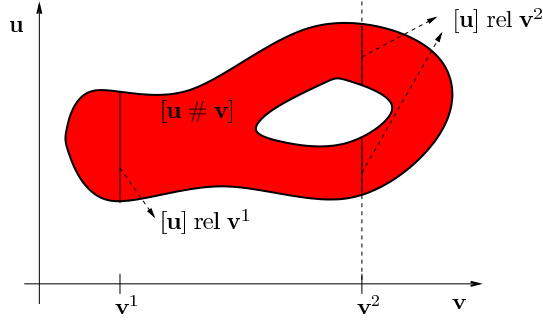


Figure 3.1. Relative braid classes and there fibers.

Definition 3.3. A relative braid class $[\mathbf{u} \# \mathbf{v}]$ is called proper if for every fiber $[\mathbf{u}'] \text{ rel } \mathbf{v}'$, with $\mathbf{v}' \in \pi([\mathbf{u} \# \mathbf{v}])$, it holds that $\text{cl}([\mathbf{u}'] \text{ rel } \mathbf{v}') \cap (\Sigma_- \text{ rel } \mathbf{v}') = \emptyset$. If $[\mathbf{u} \# \mathbf{v}]$ is not proper it is called improper.

For each fiber of a bounded proper relative braid class $[\mathbf{u} \# \mathbf{v}]$ we define a topological invariant. Fix a fiber $[\mathbf{u}'] \text{ rel } \mathbf{v}'$, with $\mathbf{v}' \in \pi([\mathbf{u} \# \mathbf{v}])$ and let $N = \text{cl}([\mathbf{u}'] \text{ rel } \mathbf{v}')$. By assumption N is compact and $\partial N \cap (\Sigma_- \text{ rel } \mathbf{v}') = \emptyset$. Then the exit set $N^- \subset \partial N$ is defined as follows: for each $\mathbf{u}' \in \partial N$ there exists a small enough neighborhood W in $\overline{\mathcal{D}}_d^n$ such that $W \setminus \Sigma \text{ rel } \mathbf{v}'$ consists of finitely many components W_j . Set $W_0 = W \cap N$, then

$$N^- := \text{cl}\{\mathbf{u}' \in \partial N \mid |W_0|_{\text{word}} \geq |W_j|_{\text{word}}, \forall j > 0\},$$

where $|\cdot|_{\text{word}}$ is the number of intersections of \mathbf{u}' with \mathbf{v}' . For a fiber $[\mathbf{u}'] \text{ rel } \mathbf{v}'$ there are finitely many components (N_i, N_i^-) . Now define the index $\mathbf{h}(\mathbf{u}' \text{ rel } \mathbf{v}') = \bigvee_i [N_i/N_i^-]$, where $[N_i, N_i^-]$ denotes the homotopy type of the pointed space $(N_i/N_i^-, [N_i^-])$. It was proved in [4] this is indeed an invariant.

Proposition 3.4. The homotopy type $\mathbf{h}(\mathbf{u}' \text{ rel } \mathbf{v}') = \bigvee_i [N_i/N_i^-]$ is independent of the fiber $[\mathbf{u}'] \text{ rel } \mathbf{v}'$ in $[\mathbf{u} \# \mathbf{v}]$. Due to Proposition 3.4 we can define

$$\mathbf{H}(\mathbf{u} \# \mathbf{v}; d) = \bigvee_i [N_i/N_i^-], \quad (3.3)$$

The homological analogue is defined as $\mathbf{CH}([\mathbf{u} \# \mathbf{v}], d) = \bigoplus_i H(N_i, N_i^-; \mathbb{Z})$. It was proved in [4] this is indeed an invariant. Proposition 3.4 was proved in [4] by associating discrete relative braids to parabolic recurrence relations.

3.2. Parabolic recurrence relations. Let \mathcal{R} be a parabolic recurrence relation (see Definition 2.1). For any braid $\mathbf{v} \in \mathcal{D}_d^m$ one can choose a parabolic recurrence relation such that all strands \mathbf{v}^k in \mathbf{v} satisfy $\mathcal{R}_i(v_{i-1}^k, v_i^k, v_{i+1}^k) = 0$, or $\mathcal{R}(\mathbf{v}) = 0$ for short. Denote by Ψ^t the local flow generated by the vector field \mathcal{R} . As such Ψ^t becomes a flow in $\overline{\mathcal{D}}_d^n$. Given a proper bounded relative braid class $[\mathbf{u} \# \mathbf{v}]$, fix a fiber $[\mathbf{u}'] \text{ rel } \mathbf{v}'$. Choose a parabolic recurrence relation such that $\mathcal{R}(\mathbf{v}') = 0$. Then, by the structure of parabolic flows the set $N = \text{cl}([\mathbf{u}'] \text{ rel } \mathbf{v}')$ is an isolating neighborhood of Ψ^t in the sense of Conley [3]. It holds that the Conley index is given by

$$h(N; \Psi^t) = \mathbf{h}(\mathbf{u}' \text{ rel } \mathbf{v}') = \bigvee_i [N_i/N_i^-].$$

Continuation properties of the Conley index yield Proposition 3.4.

A more fundamental result is that the invariant \mathbf{H} is independent of the period d in the following sense. Define the operator $\mathbf{E} : \overline{\mathcal{D}}_d^n \rightarrow \overline{\mathcal{D}}_{d+1}^n$ as follows:

$$(\mathbf{E}(\mathbf{u}))_i^k := \begin{cases} u_i^k & \text{for } i = 0, \dots, d, \\ u_d^k & \text{for } i = d + 1. \end{cases}$$

Given a bounded proper relative braid class $[\mathbf{u} \# \mathbf{v}]$ in \mathcal{D}_d^{n+m} , then $[\mathbf{E}(\mathbf{u}) \# \mathbf{E}(\mathbf{v})]$ is a bounded proper relative braid class in \mathcal{D}_{d+1}^{n+m} . The main result in [4] is:

Proposition 3.5. *It holds that $\mathbf{H}(\mathbf{u} \# \mathbf{v}; d) = \mathbf{H}(\mathbf{E}(\mathbf{u}) \# \mathbf{E}(\mathbf{v}); d + 1)$.*

One conclusion from Proposition 3.5 is that given an equivalence class of continuous positive relative braid diagrams of $[\beta(\mathbf{u}) \# \beta(\mathbf{v})]_{C^0}$, determined by the representative $\beta(\mathbf{u}) \text{ rel } \beta(\mathbf{v})$, then the index \mathbf{H} is independent of the chosen discretization d , see [4]. Therefore, one may define the topological invariant

$$\mathbf{H}(\beta(\mathbf{u}) \# \beta(\mathbf{v})) := \mathbf{H}(\mathbf{u} \# \mathbf{v}; d), \quad (3.4)$$

for any discretization d as described above. The index $\mathbf{H}(\beta(\mathbf{u}) \# \beta(\mathbf{v}))$ is an invariant for topological bounded proper relative braid classes $[\beta(\mathbf{u}) \# \beta(\mathbf{v})]_{C^0}$.

Remark 3.6. *For more details we refer to [4] where definitions of properness, boundedness, etc. for topological classes are given.*

The braid invariant \mathbf{H} has Morse theoretical implications for parabolic recurrence relations. Let Ψ^t be a parabolic flow on \mathcal{D}_d^n which fixes a skeleton $\mathbf{v} \in \mathcal{D}_d^m$ and let $[\mathbf{u} \# \mathbf{v}]$ be a bounded and proper relative braid class. If $\mathbf{H}(\beta(\mathbf{u}) \# \beta(\mathbf{v})) \neq 0$ (homotopically non-trivial), then the relative braid class $[\mathbf{u}] \text{ rel } \mathbf{v}$ has at least one fixed point for the parabolic flow, and thus a zero for the associated parabolic recurrence relation.

4. Parabolic recurrence relations for conservative systems.

4.1. Braid classes of up-down type. By Proposition 2.3 closed characteristics correspond to sequences of local minima and maxima which are zero points of a parabolic recurrence relation of up-down type. The extrema alternate in the sense that $(-1)^i(u_{i\pm 1} - u_i) > 0$ — the (natural) up-down restriction — and therefore an n -collection of extrema sequences $\{\mathbf{u}^k\}_{k=0}^{n-1}$ can be seen as a point in the space of up-down piecewise linear braid diagrams.

Definition 4.1. *The space \mathcal{E}_{2p}^n of up-down PL-braid diagrams on n strands with period $2p$ is the subset of \mathcal{D}_{2p}^n determined by the relation $(-1)^i(u_{i+1}^k - u_i^k) > 0$ for $k = 1, \dots, n$ and $i = 0, \dots, 2p - 1$. Let $\overline{\mathcal{E}}_{2p}^n$ be the subset of all braid diagrams in $\overline{\mathcal{D}}_{2p}^n$ satisfying $(-1)^i(u_{i+1}^k - u_i^k) > 0$ and as before the singular braid diagrams are defined as $\Sigma_{\mathcal{E}} = \overline{\mathcal{E}}_{2p}^n \setminus \mathcal{E}_{2p}^n$.*

The set $\overline{\mathcal{E}}_{2p}^n$ has a boundary in $\overline{\mathcal{D}}_{2p}^n$ which can be characterized as follows:

$$\partial \overline{\mathcal{E}}_{2p}^n = \{\mathbf{u} \in \overline{\mathcal{E}}_{2p}^n : u_i^k = u_{i+1}^k \text{ for at least one } i \text{ and } k\}. \quad (4.1)$$

Such braids, called horizontal singularities, are not included in Definition of $\overline{\mathcal{E}}_{2p}^n$ since the recurrence relation (2.7) does not induce a well-defined flow on the boundary $\partial \overline{\mathcal{E}}_{2p}^n$. Up-down parabolic recurrence relations therefore define a well-defined parabolic (semi-)flow Ψ^t on $\overline{\mathcal{E}}_{2p}^n$. This flow has

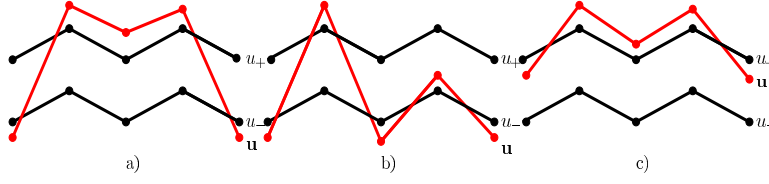


Figure 4.1. representatives of the three different relative braid classes. A fixed point in the relative braid class defined by its representative a) corresponds to the solution of the class (I), b) class (II) and c) class (III). Braid classes (a) and (b) are proper but (c) is not.

the important property that $\overline{\mathcal{E}}_{2p}^n$ is forward invariant with respect to Ψ^t , i.e. $\Psi^t(\overline{\mathcal{E}}_{2p}^n) \subset \overline{\mathcal{E}}_{2p}^n$ for all $t \geq 0$. The properties can be summarized as follows (see [4]).

Lemma 4.2. *Let Ψ^t be a parabolic flow of up-down type on $\overline{\mathcal{E}}_{2p}^n$.*

- (a) *For each point $\mathbf{u} \in \Sigma_{\mathcal{E}} - \Sigma_{\mathcal{E}}^-$, the local orbit $\{\Psi^t(\mathbf{u}) : t \in [-\epsilon, \epsilon]\}$ intersects $\Sigma_{\mathcal{E}}$ uniquely at \mathbf{u} for all ϵ sufficiently small.*
- (b) *For any such \mathbf{u} , the word metric of the braid diagram $\Psi^t(\mathbf{u})$ for $t > 0$ is strictly less than that of the diagram $\Psi^t(\mathbf{u})$, $t < 0$.*
- (c) *The flow blows up in a neighborhood of $\partial\overline{\mathcal{E}}_{2p}^n$ in such a manner that the vector field points into $\overline{\mathcal{E}}_{2p}^n$.*
- (d) *The flow is forward invariant: $\Psi^t(\overline{\mathcal{E}}_{2p}^n) \subset \overline{\mathcal{E}}_{2p}^n$ for all $t \geq 0$.*

The boundary $\partial\overline{\mathcal{E}}_{2p}^n$ can be regarded as a repelling set.

If v is a closed characteristic of a second order Lagrangian system, then its sequence of extrema $\mathbf{v} = \{v_i\}$ is a zero of the associated parabolic recurrence relation (up-down) \mathcal{R} and thus a fixed point for parabolic flow Ψ^t generated by \mathcal{R} . In the case of braids with the up-down restriction we can again define braid classes and relative braid classes, see [4]. Define the space of relative braids of up-down type

$$\mathcal{E}_{2p}^{n,m} = \{(\mathbf{u}, \mathbf{v}) \in \mathcal{E}_{2p}^n \times \mathcal{E}_{2p}^m \mid \mathbf{u} \cup \mathbf{v} \in \mathcal{E}_{2p}^{n+m}\}.$$

Elements in this space are again denoted by $\mathbf{u} \# \mathbf{v}$ and the connected components, or relative braid classes, by $[\mathbf{u} \# \mathbf{v}]_{\mathcal{E}}$. The space of relative braids with a fixed skeleton $\mathbf{v} \in \mathcal{E}_{2p}^m$ is denoted by $\mathcal{E}_{2p}^n \text{ rel } \mathbf{v}$. The fibers in $[\mathbf{u} \# \mathbf{v}]_{\mathcal{E}}$ for a fixed skeleton $\mathbf{v}' \in \pi([\mathbf{u} \# \mathbf{v}]_{\mathcal{E}})$ are denoted by $[\mathbf{u}']_{\mathcal{E}} \text{ rel } \mathbf{v}' \subset \mathcal{E}_{2p}^n \text{ rel } \mathbf{v}'$. The notions of boundedness and properness are defined in the same way, see [4]. Figure 4.1 shows the three different braid classes which correspond to the three classes of solutions as defined in Definition 1.1. The first two braid classes are proper and the third one is not. All these braid classes are obviously unbounded. It was shown in [14, 4] how to use properties of Equation (1.1) to find extra skeletal strands which make the class bounded.

Parabolic recurrence relations of up-down type and the associated braid classes satisfy an important universality principle. Let Ψ^t fix a skeleton $\mathbf{v} \in \mathcal{D}_d^m$ and let $[\mathbf{u} \# \mathbf{v}]_{\mathcal{E}}$ be a bounded and proper relative braid class. Then $N_{\mathcal{E}} := \text{cl}([\mathbf{u}]_{\mathcal{E}} \text{ rel } \mathbf{v})$ is an isolating neighborhood in the sense of Conley and therefore its Conley index $h(N_{\mathcal{E}}; \Psi^t)$ is well-defined. Define the *extended* skeleton $\mathbf{v}^* = \mathbf{v} \cup \mathbf{v}^+ \cup \mathbf{v}^-$, where

$$v_i^+ = \max_{k,i} v_i^k + 1 + (-1)^{i+1} \quad \text{and} \quad v_i^- = \min_{k,i} v_i^k - 1 + (-1)^{i+1}$$

are additional strands running above and below the original skeleton. The following crucial property was proved in [4].

Proposition 4.3. *It holds that $h(N_{\mathcal{E}}; \Psi^t) = \mathbf{H}(\beta(\mathbf{u}) \# \beta(\mathbf{v}^*))$.*

If $\mathbf{H}(\beta(\mathbf{u}) \# \beta(\mathbf{v}^*)) \neq 0$ (homotopically non-trivial), then the relative braid class $[\mathbf{u}]_{\mathcal{E}} \text{ rel } \mathbf{v}$ has at least one fixed point for the parabolic flow, and thus a zero for the associated parabolic recurrence relation of up-down type. In [4] it was also proved that this Proposition 4.3 can also be used in the setting of braid invariants for up-down type relative braid classes. In the up-down case we can define $\mathbf{H}(\mathbf{u} \# \mathbf{v}, \mathcal{E}; 2p)$, and Proposition 4.3 implies that $\mathbf{H}(\mathbf{u} \# \mathbf{v}, \mathcal{E}; 2p) = \mathbf{H}(\mathbf{u} \# \mathbf{v}^*; 2p)$. This principle gives us a powerful tool to compute the Conley index of isolating neighborhood given by bounded proper relative braid classes of up-down type via universal braid class invariants.

4.2. Fourth order equations. Let us go back now to the classification of solutions of Equation (1.1) and relate the three classes of solutions in Figure 1.1 to braid classes and put them in the context of the definitions presented in this section. The three classes of solutions are distinguished according to their intersections with the constant solutions $u_{\pm} = \pm 1$. The most straightforward way of relating a solution to a relative braid class is to take the two constant strands ± 1 as a skeleton and define the relative braid class by the free strand \mathbf{u} which intersects the constant strands ± 1 in the same manner as the solution u intersects u_{\pm} . However, the solutions $u_{\pm} = \pm 1$ lie in the *singular* energy level $E = 0$, complicating matters. In particular, the flow Ψ^t is well-defined only for the braids with up-down restriction.

We can take two different approaches to overcome this hurdle. Instead of taking the constant strands we may use the skeleton $\mathbf{v} = \mathbf{u}_+ \cup \mathbf{u}_-$, where the strands \mathbf{u}_{\pm} correspond to the solutions of Equation (1.1) which oscillate around u_{\pm} with a small amplitude on a slightly positive energy level, and finish the arguments by carefully taking limits where the amplitude of the small oscillations tends to zero and the limit solutions lie in the energy level $E = 0$, cf. [4]. Alternatively, and this is the method used in the present paper (and in [13]), one can analyze the singular energy level by using oscillating, but non-periodic, solutions near ± 1 in the skeleton. This will be explained in detail in Section 5.1. We first take a more global perspective and explain some of the ideas for simpler examples.

According to [4] the braid invariant \mathbf{H} for any braid class corresponding to a solution of the first class is non-trivial. Conley index theory then guarantees the existence of a fixed point for Ψ^t in this class. A fixed point in this braid class corresponds to the solution of Equation (1.1) of the first class. Thus there are many different solutions of the first class and their bifurcation branches exist for all $\alpha \geq 0$. In the third case the braid class is not proper (not an isolating neighborhood), since the free strand can collapse on a skeletal strand \mathbf{u}_+ . Using the information about the flow Ψ^t near the strand \mathbf{u}_+ , one can perturb the parabolic recurrence relation on a neighborhood of the boundary of the improper braid class $[\mathbf{u}]_{\mathcal{E}} \text{ rel } \mathbf{v}$ and construct some new fixed strands which will make the class proper without changing the invariant set inside the class. We refer to [12] for a detailed analysis of this case.

For the second class the braid invariant \mathbf{H} is trivial and thus does not provide information about fixed points. However, if we know that there exists a non-degenerate (hyperbolic) solution of the second class then it corresponds to a fixed point in the braid class with a trivial Conley index.

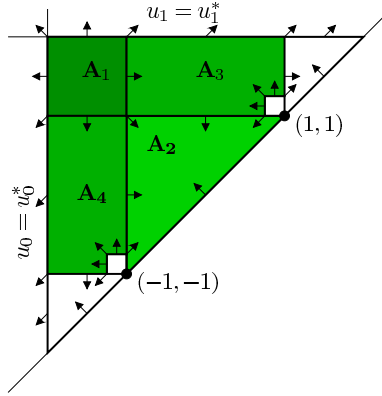


Figure 4.2. The triangle $D = I \times I \setminus \{u_1 > u_0\}$. The arrows denote (schematically) the direction of the gradient ∇W_2 . Clearly W_2 has a minimum on A_1 and maximum on A_2 . Additionally if equilibrium points ± 1 are saddle-foci then direction of ∇W_2 in a small neighborhood of $+1$ (-1) is depicted.

Hence there must be another fixed point in this class which corresponds to a different solution of the same class. This explains that the bifurcation curves form loops in Figure 1.1. In order to have an idea how to treat this case we consider the following examples.

The most straightforward way of forcing is using an already known solution(s) to prove existence of a different solution. We demonstrate this idea for Equation (1.1).

Example 4.4. Here we show that the constant solutions $u_{\pm} = \pm 1$ force the existence of periodic solutions with one minimum and one maximum per period, cf. [14]. The previous section shows that finding a periodic solution with two extremal points per period at the energy level zero is equivalent to finding a critical point of

$$W_2(u_0, u_1) = S_0(u_0, u_1) + S_0(u_1, u_0).$$

Figure 4.2 denotes the direction of the gradient ∇W_2 on the triangle $D = I \times I \cap \{u_1 > u_0\}$ where $I = [u_0^*, u_1^*]$. The system generated by (1.1) is dissipative, i.e. we can choose $u_0^* < u_1^*$ in such a way that $\partial_{u_0} W_2(u_0^*, u_1) < 0$ for all $u_1 \in (u_0^*, u_1^*)$ and $\partial_{u_1} W_2(u_0, u_1^*) > 0$ for all $u_0 \in [u_0^*, u_1^*)$, see [14]. Define $A_1 = D \cap \{u_0 < -1, u_1 > 1\}$ and $A_2 = \{-1 < u_0 < u_1 < 1\}$. The gradient of W_2 points outwards on ∂A_1 and inwards on ∂A_2 . Thus W_2 attains a local maximum on A_2 and a local minimum on A_1 . This proves the existence of two different solutions of (1.1). We note that one of them intersects neither u_+ nor u_- . The other one is in the class $[\sigma_1^2 \sigma_2^2, 2]$ and hence intersects both u_+ and u_- . Actually, ∇W_2 is not defined for $u_0 = u_1$ but by slightly shrinking the set A_2 we obtain the previous result. In the parameter range $\alpha \in [0, \sqrt{8})$ in which case the stationary solutions u_{\pm} are saddle-foci, the sets A_3 and A_4 depicted in Figure 4.2 are isolating neighborhoods with respect to the gradient flow of W_2 , see [14] for more details. The Conley indices of A_3 and A_4 are non-trivial. Hence there is a critical point of W_2 in both isolating neighborhoods A_3 and A_4 . These critical points correspond to solutions of the class $[\sigma_2^2, 2]$, respectively $[\sigma_1^2, 2]$.

We explicitly used known solutions to prove existence of geometrically different ones. However, as we mentioned in the introduction, forcing can be considered in a more general framework.

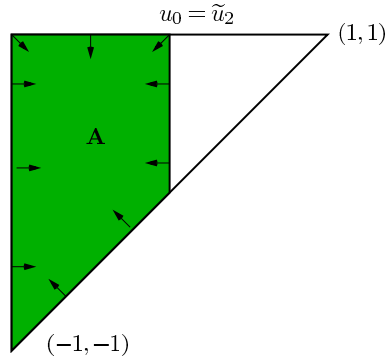


Figure 4.3. The triangle $D = [-1, 1] \times [-1, 1] \setminus \{u_1 > u_0\}$. The arrows denote (schematically) the direction of the gradient ∇W_2 . Clearly W_2 has a maximum on A .

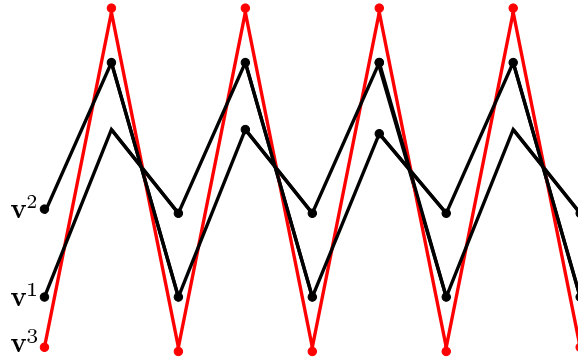


Figure 4.4. Sketch of the strands v^1, v^2 and v^3 .

Instead of using explicitly known solution(s) one can ask the following question. When does existence of a solution $\tilde{u} \in [\sigma, p]$ force existence of some other solution? The next example presents the basic ideas of this approach.

Example 4.5. Let \tilde{u} be a solution of the class $[\sigma_1^2 \sigma_2^4, 2]$. Then \tilde{u} has four non-degenerate extremal points per period with $\tilde{u}_0 < -1 < \tilde{u}_2 < 1 < \tilde{u}_1, \tilde{u}_3$, see Figure 1.2. Let us consider 2-periodic sequences (u_0, u_1) in $A = \{-1 < u_0 < u_1 < 1\} \cap \{u_0 < \tilde{u}_2\}$. According to the previous section $\mathcal{R}_1(u_1, \tilde{u}_2, u_3) < \mathcal{R}_1(\tilde{u}_1, \tilde{u}_2, \tilde{u}_3) = 0$ for $u_1 < \tilde{u}_1$ and $u_3 < \tilde{u}_3$. Hence, for $(\tilde{u}_2, u_0) \in \partial A$ it holds that

$$\partial_1 W_2(\tilde{u}_2, u_1) = \partial_2 S_0(u_1, \tilde{u}_2) + \partial_1 S_0(\tilde{u}_2, u_1) = \mathcal{R}_1(u_1, \tilde{u}_2, u_1) < 0.$$

As before the gradient ∇W_2 points inward on ∂A and W_2 attains a local maximum on A , see Figure 4.3. This maximum corresponds to a solution u of (1.1) with two extremal points per period satisfying $-1 < \min\{u(t), t \in \mathbb{R}\} < \tilde{u}_2 < 1$ and $-1 < \max\{u(t), t \in \mathbb{R}\} < 1$.

We studied W_2 to force the existence of periodic solutions with two extremal points per period. In order to force existence of general periodic solutions we need to study the gradient flow generated by W_{2p} , for $p > 1$.

Example 4.6. Let $\tilde{u} \in [\sigma_1^2 \sigma_2^4, 4]$ with the sequence of extrema $\{\tilde{u}_i\}$. For an arbitrary $p \in \mathbb{N}$ let $\mathbf{v}^1 \cup \mathbf{v}^2 \in \mathcal{E}_{2p}^2$, be defined by $v_i^1 = \tilde{u}_i$ and $v_i^2 = \tilde{u}_{(i+2) \bmod 2p}$. The system generated by (1.1) is dissipative and we can choose $I = [u_0^*, u_1^*]$ where the constants u_0^*, u_1^* are such that $u_0^* < v_i^1, v_i^2 < u_1^*$ and $\mathcal{R}_i(u_{i-1}, u_0^*, u_{i+1}) > 0$ while $\mathcal{R}_i(u_{i-1}, u_1^*, u_{i+1}) < 0$ for $u_{i\pm 1} \in I$. Define

$$\Omega_i = \begin{cases} \{(u_{i-1}, u_i, u_{i+1}) \in I^3 \mid u_0^* \leq u_{i\pm 1} \leq u_i \leq u_1^*\}, & i \text{ odd,} \\ \{(u_{i-1}, u_i, u_{i+1}) \in I^3 \mid u_0^* \leq u_i \leq u_{i\pm 1} \leq u_1^*\}, & i \text{ even.} \end{cases}$$

Denote by Ω_{2p} the set of $2p$ periodic sequences $\{u_i\}$ for which $(u_{i-1}, u_i, u_{i+1}) \in \Omega_i$. Furthermore define the set

$$C := \{\mathbf{u} \in \Omega_{2p} : \iota(\mathbf{u}, \mathbf{v}^1) = \iota(\mathbf{u}, \mathbf{v}^2) = 2p\},$$

where $\iota(\mathbf{u}, \mathbf{v}^1)$ is the number of intersections of the sequence $\{u_i\}_{i=0}^{2p}$ and $\{v_i^1\}_{i=0}^{2p}$. Since $\iota(\mathbf{v}^1, \mathbf{v}^2) = p < 2p$ and the system is dissipative, the vector field \mathcal{R} is transverse to ∂C . We note that C is disjoint from the singular ‘‘diagonal’’ $u_i = u_{i\pm 1}$. Moreover, the set C is contractible, compact, and \mathcal{R} is pointing outward at the boundary of ∂C . The set C is therefore negatively invariant for the induced parabolic flow Ψ^t and there exists a global minimum \mathbf{v}^3 of W_{2p} which is a fixed point of Ψ^t in the interior of C . Figure 4.4 depicts the strands $\mathbf{v}^1, \mathbf{v}^2$ and \mathbf{v}^3 .

5. Forcing solutions in $[\sigma_1^2 \sigma_2^{2p}, p]$. In this section we prove the existence of geometrically distinct solutions of Equation (1.1) of the class $[\sigma_1^2 \sigma_2^{2p}, p]$ under the assumption that there exists a solution $\tilde{u} \in [\sigma_1^2 \sigma_2^4, 2]$. For the remainder of this section we assume the flow Ψ^t generated by \mathcal{R} associated to Equation (1.1). The Conley index of a relative braid class can be used to detect the existence of a fixed point of Ψ^t within the braid class. However this method works only for a proper bounded braid class $[\mathbf{u}]_{\mathcal{E}} \text{ rel } \mathbf{w}$ whose skeleton \mathbf{w} is a fixed point of the flow Ψ^t (zero point of \mathcal{R}). In our case, it is tempting to use the solutions $u_{\pm} = \pm 1$ as strands in the skeleton, but they do not satisfy the required up-down restriction, hence the flow Ψ^t is singular at points with coordinates $u_i = \pm 1$. To overcome this problem we use the sequence $\{u_i^{\varepsilon}\}_{i=0}^{\infty}$ given by the following lemma to define an isolating neighborhood M as a subset of some proper and bounded braid class $[\mathbf{u}]_{\mathcal{E}} \text{ rel } \mathbf{w}$. Finally we will show that the homological Conley index of the isolating neighborhood M is the same as $\mathbf{H}(\mathbf{u} \# \mathbf{w}, \mathcal{E}; 2p)$, or $\mathbf{H}(\mathbf{u} \# \mathbf{w}^*, 2p)$.

5.1. Construction of braid classes. The following lemma establishes small oscillating solutions around $u = \pm 1$.

Lemma 5.1. (see [13]) Let $-\sqrt{8} < \alpha < \sqrt{8}$. For any $\varepsilon > 0$ there exists a sequence $\{u_i^{\varepsilon}\}_{i=0}^{\infty}$,

$$0 < (-1)^{i+1}(u_i^{\varepsilon} - 1) < \varepsilon,$$

which satisfies $\mathcal{R}_i(u_{i-1}^{\varepsilon}, u_i^{\varepsilon}, u_{i+1}^{\varepsilon}) = 0$, for all $i \geq 1$.

In what follows, when considering a braid class in \mathcal{E}_{2p} we will use, among others, a skeletal strand $(u_0^{\varepsilon}, \dots, u_{2p-1}^{\varepsilon})$. This strand does not close up at $i = 2p = 0 \bmod 2p$, i.e. $R_0(u_{2p-1}^{\varepsilon}, u_0^{\varepsilon}, u_1^{\varepsilon}) \neq 0$, but this will not lead to undesirable effects, as we shall see later.

The symmetry of Equation (1.1) enforces an analogous result near $u_- = -1$. To be explicit, let $\overline{u}_i^{\varepsilon} = -u_{i+1}^{\varepsilon}$. At $u = -1$ we use the solution (compare [13])

$$\widehat{u}_i^{\varepsilon} = \overline{u}_{i-2 \bmod 2p}^{\varepsilon},$$

i.e. $\widehat{u}_i^\varepsilon = \overline{u}_{i-2}^\varepsilon$ for $i = 2, \dots, 2p$, $\widehat{u}_0^\varepsilon = \overline{u}_{2p-1}^\varepsilon$, and $\widehat{u}_1^\varepsilon = \overline{u}_{2p}^\varepsilon$. Note that $\widehat{u}_i^\varepsilon$ does not close at $i = 2$.

In order to find geometrically distinct solutions we define a braid class $[\mathbf{u}^I]_\varepsilon \text{ rel } \mathbf{w} \in \mathcal{E}_{2p}^1 \text{ rel } \mathbf{w}$ for every

$$I = \{j_1, j_2, \dots, j_n\} \in \mathbb{N}^n, \quad (5.1)$$

satisfying

$$1 < j_1 < j_2 < \dots < j_n < p - 1. \quad (5.2)$$

We start with identifying the skeletal strands

$$\mathbf{w} = \mathbf{v}^1 \cup \mathbf{v}^2 \cup \mathbf{v}^3 \cup \mathbf{v}^4 \cup \mathbf{v}^5 \cup \mathbf{v}^6. \quad (5.3)$$

The strand \mathbf{v}^1 corresponds to a sequence of extrema $\{\tilde{u}_i\}$ of the solution $\tilde{u} \in [\sigma_1^2 \sigma_2^4, 2]$, i.e. $v_i^1 = \tilde{u}_i$. The strand \mathbf{v}^2 is a shift of the strand \mathbf{v}^1 given by $v_i^2 = v_{(i \bmod 4)+2}^1$. We may assume that $v_1^1 \leq v_2^1$, otherwise interchange \mathbf{v}_1 and \mathbf{v}_2 . The strand \mathbf{v}^3 corresponds to the sequence of extrema of the solution obtained in Example 4.6. It holds that $v_{2i}^3 < \min\{v_{2i}^1, v_{2i}^2\}$ and $v_{2i+1}^3 > \max\{v_{2i+1}^1, v_{2i+1}^2\}$ for all i . The strand \mathbf{v}^4 is defined by the sequence of extrema of the solution constructed in Example 4.5 and $-1 < v_{2i}^4 < \tilde{u}_2$ while $-1 < v_{2i+1}^4 < 1$. All the strands defined up to now are fixed points of Ψ^t . Finally, we define the strands \mathbf{v}^5 and \mathbf{v}^6 by $v_i^5 = 1 + (-1)^{i+1} \varepsilon_0$ and $v_i^6 = -1 + (-1)^{i+1} \varepsilon_0$, where

$$\varepsilon_0 = \frac{1}{2} \min\{|u_i^\varepsilon - 1|, i = 0, \dots, 2p - 1\}.$$

and

$$\varepsilon = \frac{1}{2} \min\{-1 - \tilde{u}_0, \tilde{u}_1 - 1, 1 - \tilde{u}_2, \tilde{u}_3 - 1, 1 + v_0^4, \dots, 1 + v_{2p-1}^4\},$$

The strands \mathbf{v}^5 and \mathbf{v}^6 are *not* fixed points of Ψ^t . We postpone discussing the relation of \mathbf{v}^5 and \mathbf{v}^6 with the solutions u_i^ε and $\widehat{u}_i^\varepsilon$ (see §5.2 below). First we describe how the set I defines the braiding of a free strand \mathbf{u} with the skeletal strands \mathbf{v}^1 and \mathbf{v}^2 .

Definition 5.2. *The braid class $[\mathbf{u}^I]_\varepsilon \text{ rel } \mathbf{w} \subset \mathcal{E}_{2p}^1 \text{ rel } \mathbf{w}$ is defined by its representative \mathbf{u}^I satisfying:*

1. $u_0^I \in (v_0^1, v_0^6)$,
2. $u_{2i+1}^I \in (v_1^5, v_1^1)$ for all i ,
3. $u_{2i}^I \in \begin{cases} (v_2^4, v_2^1) & : \text{ if } i \in I, \\ (v_2^1, v_2^5) & : \text{ if } i \neq 0 \text{ and } i \notin I. \end{cases}$

The points u_{2i}^I are thus lower for $i \in I$ than for $i \notin I$, and these are called the ‘‘fingers’’, see Figure 1.5.

As said before, the skeleton \mathbf{w} is not a fixed point of Ψ^t (only four out of six strands are fixed). The braid class $[\mathbf{u}^I]_\varepsilon \text{ rel } \mathbf{w}$ however is proper and bounded. Suppose that Φ^t is an arbitrary parabolic flow of up-down type such that $\Phi^t(\mathbf{w}) = \mathbf{w}$. Then, the set

$$N_{I,\varepsilon} := \{\mathbf{u} \in \text{cl}([\mathbf{u}^I]_\varepsilon \text{ rel } \mathbf{w}) : (-1)^i (u_{i+1} - u_i) \geq \delta \quad \forall i\} \quad (5.4)$$

is an isolating neighborhood of the flow Φ^t , for $\delta > 0$ sufficiently small (immediately suppressing the dependence of $N_{I,\varepsilon}$ on δ). Moreover, by Proposition 4.3, $h(N_{I,\varepsilon}, \Phi^t) = \mathbf{H}(\mathbf{u}^I \# \mathbf{w}, \varepsilon; 2p)$.

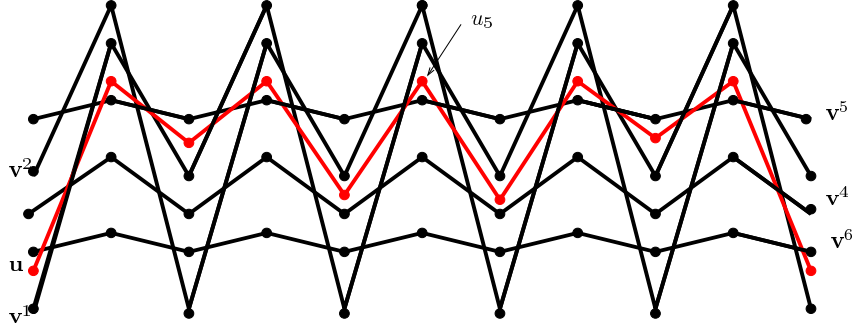


Figure 5.1. A representative of the braid class $[\mathbf{u}]_{\mathcal{E}} \text{ rel } \mathbf{w}_{\epsilon} \subset \mathcal{E}_{10}^1 \text{ rel } \mathbf{w}$, with $I = \{2, 3\}$. To keep the figure synoptical we do not display the skeletal strand \mathbf{v}^3 , which crosses all the other skeletal strands in between each two anchor points and makes the braid class bounded. Notice that there would be no upper bound for u_5 without this strand \mathbf{v}^3 . There are “fingers” at $i = 4$ and $i = 6$.

We denote by $N_{I,\epsilon}^-$ the subset of $\partial N_{I,\epsilon}$ where the flow Φ^t points out of the set $N_{I,\epsilon}$. The set $N_{I,\epsilon}^-$ is the same for every flow Φ^t that fixes the skeleton \mathbf{w} . Note that $N_{I,\epsilon}^-$ contains those pieces of the boundary where $u_i^I = v_i^5$ ($i = 1, \dots, 2p - 1$) or $u_0^I = v_0^6$. The non-triviality of $\mathbf{H}(\mathbf{u}^I \# \mathbf{w}, \mathcal{E}; 2p)$ is given by the following theorem, which is proved in Section 6.

Theorem 5.3. *The homology of $\mathbf{H}(\mathbf{u}^I \# \mathbf{w}, \mathcal{E}; 2p)$ is given by:*

$$H_k(\mathbf{H}(\mathbf{u}^I \# \mathbf{w}, \mathcal{E}; 2p)) = \begin{cases} \mathbb{Z}, & \text{if } k = 2p - \#I, \\ 0, & \text{otherwise,} \end{cases} \quad (5.5)$$

where $\#I$ is the number of elements in I .

A fundamental step in the proof of Theorem 5.3 is the following observation. The set of ‘fingers’ I can be decomposed in subsets which contain consecutive fingers. The relative braid class $[\mathbf{u}^I]_{\mathcal{E}} \text{ rel } \mathbf{w} \subset \mathcal{E}_{2p}^1 \text{ rel } \mathbf{w}$ has a product structure with respect to this decomposition. This allows us to compute \mathbf{H} for the separate pieces. In Section 6 we will describe this procedure in detail and calculate \mathbf{H} for the individual pieces, which then proves the general statement in Theorem 5.3.

5.2. Isolating neighborhoods for Equation (1.1). We now construct an isolating neighborhood $M_{I,\epsilon}$ for Ψ^t generated by Equation (1.1) whose Conley index can be computed via the braid invariant $\mathbf{H}(\mathbf{u}^I \# \mathbf{w}, \mathcal{E}; 2p)$.

Definition 5.4. *Let $M_{I,\epsilon}$ be a subset of $N_{I,\epsilon}$ (defined in (5.4)) such that $\mathbf{u} \in M_{I,\epsilon}$ if and only if*

1. $u_0 < \widehat{u}_0^\epsilon$,
2. $(-1)^i u_i < (-1)^i u_i^\epsilon$, for all i .

We denote by $M_{I,\epsilon}^-$ the subset of $\partial M_{I,\epsilon}$ where the flow Ψ^t points out of the set $M_{I,\epsilon}$.

Lemma 5.5. *For sufficiently small $\epsilon > 0$ the set $M_{I,\epsilon}$ is an isolating neighborhood for the flow Ψ^t . Moreover, $H_*(M_{I,\epsilon}, M_{I,\epsilon}^-) = H_*(\mathbf{H}(\mathbf{u}^I \# \mathbf{w}, \mathcal{E}; 2p))$.*

Proof. Consider points $\mathbf{u} \in \partial M_{I,\epsilon}$ characterized by $u_0 = \widehat{u}_0^\epsilon$. Using the recurrence relation \mathcal{R} we can study the behavior of Ψ^t at these points. The monotonicity of \mathcal{R} combined with Lemma 5.1 implies that

$$\mathcal{R}_0(u_{2p-1}, \widehat{u}_0^\epsilon, u_1) > \mathcal{R}_0(\widehat{u}_{2p-1}^\epsilon, \widehat{u}_0^\epsilon, \widehat{u}_1^\epsilon) = 0,$$

and the flow Ψ^t thus points out of the set $M_{I,\epsilon}$. Analogously

$$(-1)^i \mathcal{R}_i(u_{i-1}, u_i^\epsilon, u_{i+1}) < (-1)^i \mathcal{R}_i(u_{i-1}^\epsilon, u_i^\epsilon, u_{i+1}^\epsilon) = 0,$$

on the codimension 1 boundaries where $u_i = u_i^\epsilon$ and $u_{i\pm 1} \neq u_{i\pm 1}^\epsilon$. The flow thus points out of $M_{I,\epsilon}$ also at these boundary points. As in the proof of Lemma 40 in [4] the flow is transversal at the rest of the boundary $\partial M_{I,\epsilon}$ provided that $\epsilon > 0$ is sufficiently small. We note that $\partial M_{I,\epsilon}$ intersects neither $u_0 = u_0^\epsilon$ nor $u_2 = \widehat{u}_2^\epsilon$, hence the fact that we do have information on the direction of the flow on these hyperplanes (since the strands u^ϵ and \widehat{u}^ϵ do not “close” at coordinates $i = 0$ and $i = 2$, respectively) causes no problems.

To relate $H_*(M_{I,\epsilon}, M_{I,\epsilon}^-)$ to $H_*(\mathbf{H}(\mathbf{u}^I \# \mathbf{w}, \mathcal{E}; 2p))$ we show that the pair $(M_{I,\epsilon}, M_{I,\epsilon}^-)$ is homotopic to $(N_{I,\epsilon}, N_{I,\epsilon}^-)$. Then

$$H_*(M_{I,\epsilon}, M_{I,\epsilon}^-) \cong H_*(N_{I,\epsilon}, N_{I,\epsilon}^-) \cong H_*(\mathbf{H}(\mathbf{u}^I \# \mathbf{w}, \mathcal{E}; 2p)).$$

Define $g = (g_0, \dots, g_{2p-1}) : N_{I,\epsilon} \times [0, 1] \rightarrow M_{I,\epsilon}$ as follows

$$g_0(\mathbf{u}, t) = \begin{cases} u_0, & \text{if } u_0 < \widehat{u}_0^\epsilon, \\ (1-t)u_0 + t\widehat{u}_0^\epsilon, & \text{otherwise,} \end{cases}$$

and

$$g_i(\mathbf{u}, t) = \begin{cases} u_i, & \text{if } (-1)^i u_i < (-1)^i u_i^\epsilon, \\ (1-t)u_i + t u_i^\epsilon, & \text{otherwise,} \end{cases}$$

for $i > 0$, where $\mathbf{u} = (u_0, \dots, u_{2p-1})$. It is straightforward to check that g is a homotopy between $N_{I,\epsilon}$ and $M_{I,\epsilon}$.

If $\mathbf{u} \in N_{I,\epsilon}$ and $u_i = v_0^6$ or $u_i = v_i^5$ for some i , then $\mathbf{u} \in N_{I,\epsilon}^-$. On the other hand for $\mathbf{u} \in M_{I,\epsilon}$ such that $u_i = \widehat{u}_0^\epsilon$ or $u_i = u_i^\epsilon$ for some i it holds that $\mathbf{u} \in M_{I,\epsilon}^-$. We conclude that $g|_{N_{I,\epsilon}^-}$ is a homotopy between $N_{I,\epsilon}^-$ and $M_{I,\epsilon}^-$. ■

The fact that $H_*(\mathbf{H}(\mathbf{u}^I \# \mathbf{w}, \mathcal{E}; 2p))$ is non-trivial for the braid classes described above implies that the parabolic flow Ψ^t generated by Equation (1.1) has many geometrically distinct solutions of various braid classes provided a solution $\tilde{u} \in [\sigma_1^2 \sigma_2^4, 2]$ exists. This proves the ordering relation $[\sigma_1^2 \sigma_2^4, 2] < [\sigma_1^2 \sigma_2^{2p}, p]$. The different solutions can be characterized by different ‘fingers’ (see Figure 5.1). A simple count gives a lower bound on the number of geometrically distinct solutions. Indeed, fingers cannot occur at $i = 0, 2, 2p - 2$, which leaves $p - 3$ slots, and therefore the lower bound is given by $\beta_{p,p} = 2^{p-3}$ possibilities, proving the first part of Theorem 1.8.

6. Computation of the homological Conley index in Theorem 5.3. We start by simplifying the skeleton \mathbf{w} without changing the Conley index. According to Proposition 3.4 the index \mathbf{H} is invariant under homotopies of the skeleton \mathbf{w} . The skeletal strands \mathbf{v}^5 and \mathbf{v}^6 can be deformed to the constant strands $+1$ and -1 without changing the index \mathbf{H} . By the same token we can impose symmetry upon \mathbf{v}^1 (and thus \mathbf{v}^2) by assuming deforming \mathbf{v}^1 (\mathbf{v}^2) to a configuration for which $v_1^1 = v_1^2 = v_3^1 = v_3^2$. Finally, omitting the skeletal strand \mathbf{v}^4 does not change the index either (since \mathbf{v}^4 can be contracted onto -1 , whereas the free strand cannot). Compare Figure 5.1, which shows the braid class $[\mathbf{u}^I]_{\mathcal{E}} \text{ rel } \mathbf{w}$ for $I = \{2, 3\}$. Figure 6.2 depicts the corresponding class with the simplified skeleton. From now on $[\mathbf{u}^I] \text{ rel } \mathbf{w}$ denotes the braid class with the simplified skeleton. First we demonstrate the main ideas via three basic examples.

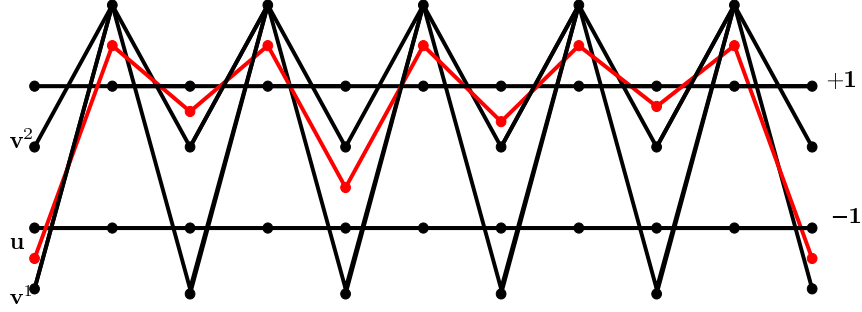


Figure 6.1. The braid class $[\mathbf{u}^I] \text{ rel } \mathbf{w} \subset \mathcal{D}_{10}^1 \text{ rel } \mathbf{w}$ for $I = \{2\}$. The skeletal strand \mathbf{v}^3 is not displayed.

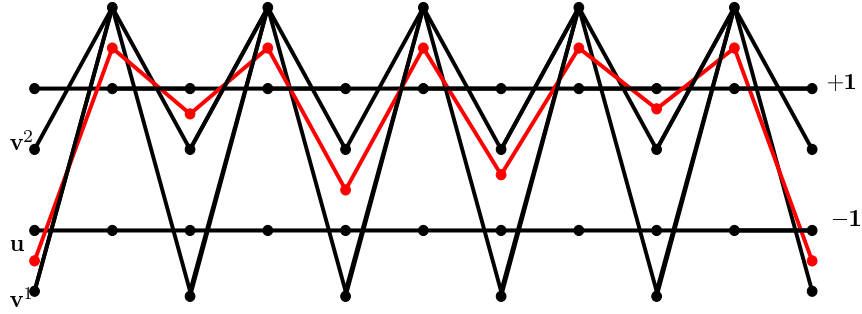


Figure 6.2. The braid class $[\mathbf{u}^I] \text{ rel } \mathbf{w} \subset \mathcal{D}_{10}^1 \text{ rel } \mathbf{w}$ for $I = \{2, 3\}$ with the simplified skeleton. To keep the figure clear we do not display the strand \mathbf{v}^3 which makes the braid class bounded.

6.1. Basic examples. **Example 6.1.** Let $p = 5$ and $I = \{2\}$. The representative of the class $[\mathbf{u}^I] \text{ rel } \mathbf{w} \subset \mathcal{D}_{10}^1 \text{ rel } \mathbf{w}$ is depicted in Figure 6.1. If $\mathbf{u} \in N_I := \text{cl}([\mathbf{u}^I] \text{ rel } \mathbf{w})$ then

$$u_i \in \begin{cases} [v_0^1, -1], & \text{if } i = 0, \\ [-1, v_2^1], & \text{if } i = 4, \\ [v_2^1, 1], & \text{if } i \text{ is even and } i \notin \{0, 4\}, \\ [1, v_1^1], & \text{if } i \text{ is odd.} \end{cases} \quad (6.1)$$

We will call the interval in which the coordinate u_i (or a collection of coordinates) must lie its configuration space. We see that $N_I \cong [0, 1]^{2p}$ and the intersection number of the free strand with the skeletal strands increases when crossing the boundary where $u_4 = -1$ or $u_4 = \tilde{u}_2$. In the case that any other anchor point different from u_4 reaches the boundary the intersection number decreases. Let $N_I^- \subset N_I$ be the set at which the intersection number decreases. Then N_I^- is the entire boundary of N_I except (the interior of) the faces $\{\mathbf{u} \in N_I : u_4 = -1\}$ and $\{\mathbf{u} \in N_I : u_4 = \tilde{u}_2\}$. By computing the relative homology $H_*(N_I, N_I^-)$ we obtain the index

$$H_k(\mathbf{H}(\mathbf{u}^I \# \mathbf{w}, 2p)) = \begin{cases} \mathbb{Z}, & \text{if } k = 2p - 1, \\ 0, & \text{otherwise.} \end{cases}$$

The same is true for $I = \{3\}$.

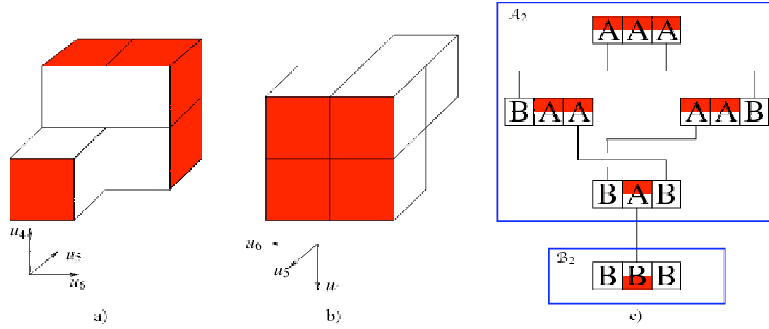


Figure 6.3. a) and b) Two views of the configuration space $U(2)$ of the anchor points (u_4, u_5, u_6) for $[u^I]$ rel \mathbf{w} with $I = \{2, 3\}$, cf. Figure 6.2 and Example 6.2. The set $U^-(2)$ consists of the faces displayed in red; c) schematic representation of $U(2)$. The shaded faces form $U^-(2)$. The cube BBB corresponds to the front cube at a). Division into A_1 and B_1 is displayed.

Example 6.2. Let $[u^I]$ rel $\mathbf{w} \subset \mathcal{D}_{10}^1$ rel \mathbf{w} with $I = \{2, 3\}$, see Figure 6.2. Again the anchor points u_i with $i \notin \{4, 5, 6\}$ are confined to the intervals defined by (6.1) and if some of them attain the boundary, then $\mathbf{u} \in N_I^-$. The configuration space of the anchor points (u_4, u_5, u_6) is given by a union of five ‘cubes’ shown in Figure 6.3(a,b). If (u_4, u_5, u_6) lies in one of the faces depicted in red then $\mathbf{u} \in N_I^-$. Note that the configuration space of the anchor points u_i with $i \notin \{4, 5, 6\}$ is independent of the position of the anchor points u_4, u_5, u_6 and vice versa. The relative homology can now be “read” from the figure (and later on we will prove it in more generality):

$$H_k(\mathbf{H}(\mathbf{u}^I \# \mathbf{w}, 2p)) = \begin{cases} \mathbb{Z}, & \text{if } k = 2p - 2, \\ 0, & \text{otherwise.} \end{cases}$$

The following example demonstrates the splitting of anchor points into blocks with the property that the configuration space of the anchor points in one block is independent of the positions of the anchor points in the different blocks.

Example 6.3. Let $[u^I]$ rel $\mathbf{w} \subset \mathcal{D}_{14}^1$ rel \mathbf{w} , where $I = \{2, 4, 5\}$, see Figure 6.4. Define $\mathcal{J}_1 = \{4\}$ and $\mathcal{J}_2 = \{8, 9, 10\}$. The configuration space of u_4 is $[-1, \tilde{u}_2]$ for any position of the other anchor points. As we saw in the previous example the configuration space of u_i with $i \in \mathcal{J}_2$ does not depend on the position of any anchor point u_j with j in the complement of \mathcal{J}_2 . Finally, for $i \in \mathcal{J}_0 = \{0, \dots, 2p\} \setminus \bar{\mathcal{J}}$, where $\bar{\mathcal{J}} = \mathcal{J}_1 \cup \mathcal{J}_2$, it holds that the configuration space of u_i is always given by (6.1).

6.2. Decomposition of the sets N_I and N_I^- . First we formalize the splitting of anchor points introduced in Example 6.3. This splitting depends on the set $I = \{j_1, j_2, \dots, j_n\}$. We remind the reader that if we work with the braid class $[u^I]$ rel $\mathbf{w} \subset \mathcal{E}_{2p}^1$ then we assume that

$$1 < j_1 < j_2 < \dots < j_n < p - 1.$$

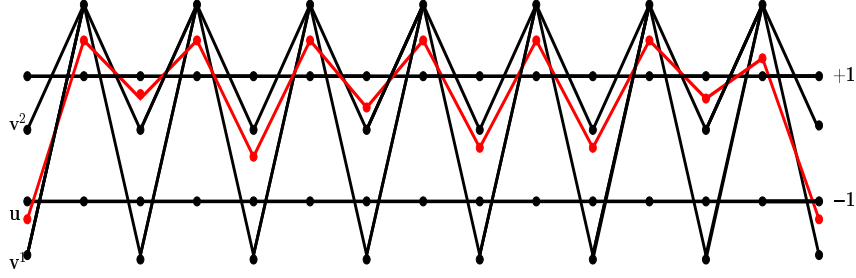


Figure 6.4. The braid class $[\mathbf{u}^I]$ rel $\mathbf{w} \in \mathcal{D}_{14}^1$ rel \mathbf{w} for $I = \{2, 4, 5\}$. The skeletal strand \mathbf{v}^3 is not displayed.

Definition 6.4. For the set $I = \{j_1, j_2, \dots, j_n\}$ we define

$$\bar{\mathcal{J}} = \{i \in \mathbb{N} : (i = 2j_k) \text{ or } (i = 2j_k + 1 \text{ and } j_{k+1} = j_k + 1) \text{ for some } k\},$$

consisting of the fingers and the points directly in between two fingers, and the complement

$$\mathcal{J}_0 = \{0, 1, \dots, 2p - 1\} \setminus \bar{\mathcal{J}}.$$

We decompose $\bar{\mathcal{J}}$ into consecutive blocks i.e.

$$\bar{\mathcal{J}} = \mathcal{J}_1 \cup \mathcal{J}_2 \cup \dots \cup \mathcal{J}_l,$$

where $\mathcal{J}_k = \{i_1^k, i_2^k, \dots, i_{p_k}^k\}$ with $i_{j+1}^k = i_j^k + 1$ for $0 < j < p_k$ and $i_{p_k}^k + 1 < i_1^{k+1}$. Notice that $\#I = \sum_{i=1}^l (\#\mathcal{J}_i + 1)/2$.

The following statement generalizes the observations from the previous examples to an arbitrary set I . If $\mathbf{u} \in N_I$ and $i \in \mathcal{J}_0$ then

$$u_i \in \begin{cases} [v_0^1, -1], & \text{if } i = 0, \\ [v_2^1, 1], & \text{if } i \text{ is even and positive,} \\ [1, v_1^1], & \text{if } i \text{ is odd.} \end{cases} \quad (6.2)$$

If u_i attains the boundary of the interval given by (6.2) then $\mathbf{u} \in N_I^-$. For every set $\mathcal{J}_m = \{i_1^m, \dots, i_{p_m}^m\}$, with $m > 0$, it holds that $i_1^m - 1, i_{p_m}^m + 1 \in \mathcal{J}_0$ and the anchor points $u_{i_1^m - 1}, u_{i_{p_m}^m + 1}$ lie in the interval given by (6.2). The fact that the configuration space of the anchor point depends only on its immediate neighbors implies that the configuration space of the anchor point u_i with $i \in \mathcal{J}_m$ depends only on the anchor points u_j with $j \in \mathcal{J}_m$. Therefore

$$N_I = U_0 \times U_1 \times \dots \times U_l, \quad (6.3)$$

where

$$U_i = \text{im}(\pi^i(N_I)),$$

and $\pi^i : N_I \rightarrow \mathbb{R}^{\#\mathcal{J}_i}$ is the projection on the coordinates with indices in \mathcal{J}_i .

Example 6.5. Let $[\mathbf{u}^I]$ rel \mathbf{w} be as in Example 6.3. Then $N_I = U_0 \times U_1 \times U_2$ with $\mathcal{J}_1 = \{4\}$ and $\mathcal{J}_2 = \{8, 9, 10\}$. The set $U_1 = [-1, \tilde{u}_2]$ and $U_2 = U(2)$ is depicted in Figure 6.3. It follows from (6.2) that U_0 is homotopic to a 10-dimensional cube. By employing the sets U_i we write

$$N_I^- = \bigcup_{j=0}^l U_0 \times U_1 \times \dots \times U_{j-1} \times U_j^- \times U_{j+1} \times \dots \times U_l, \quad (6.4)$$

where

$$U_j^- = \text{im}(\pi^j(N_{\mathcal{J}_j}^-)),$$

and $\mathbf{u} \in N_{\mathcal{J}_j}^-$ if and only if $\mathbf{u}' \in N_I^-$ for every $\mathbf{u}' \in N_I$ which satisfies $u'_i = u_i$ for $i \in \mathcal{J}_j$. In other words $N_{\mathcal{J}_j}^-$ consists of the points which are in N_I^- due to the position of the anchor points u_i with $i \in \mathcal{J}_j$. This implies that U_j^- can be determined by considering U_j only (independent of the other components of N_I).

Example 6.6. Let $I = \{2, 4, 5\}$. Then $N_I^- = U_0^- \times U_1 \times U_2 \cup U_0 \times U_1^- \times U_2 \cup U_0 \times U_1 \times U_2^-$. The set $U_1^- = \emptyset$, $U_2^- = U^-(2)$ is depicted in Figure 6.3 and $U_0^- = \partial U_0$.

Having decomposed N_I and N_I^- , we first compute the homology of the sets U_i and U_i^- . Then we derive the homology N_I and N_I^- . Finally, using the exact sequence which relates $H_*(N_I)$ and $H_*(N_I^-)$ to $H_*(N_I, N_I^-)$, we prove Theorem 5.3.

6.3. The homology of U_0 and U_0^- . It follows from (6.2) that $U_0 \cong [0, 1]^{\#\mathcal{J}_0}$ and $U_0^- \cong \partial U_0$. Summarizing

$$H_k(U_0) = \begin{cases} \mathbb{Z}, & \text{if } k = 0, \\ 0, & \text{otherwise,} \end{cases} \quad (6.5)$$

and

$$H_k(U_0^-) = \begin{cases} \mathbb{Z}, & \text{if } k = 0, \#\mathcal{J}_0 - 1 \\ 0, & \text{otherwise.} \end{cases} \quad (6.6)$$

6.4. The homology of U_i and U_i^- for $i > 0$. The symmetry of the skeleton \mathbf{w} implies that the sets U_i and U_i^- depend only on the number of elements in \mathcal{J}_i but not on their values. If $\#\mathcal{J}_i = 2m - 1$ then $U_i \simeq U(m) \subset \mathbb{R}^{2m-1}$, where $U(m)$, the universal block of length $2m - 1$, is defined to be U_1 for the set $I = \{2, 3, \dots, m + 1\}$. Therefore it is enough to deal with the sets

$$U(m) \subset \mathbb{R}^{2m-1} \quad \text{and} \quad U^-(m) \subset \mathbb{R}^{2m-1},$$

for all $m \in \mathbb{N}$. Whenever explicit coordinates are used we will identify $U(m)$ with U_1 for $I = \{2, \dots, m + 1\}$. The set $U(m)$ is a collection of cubes $\mathbf{C} = C_0 \times C_1 \times \dots \times C_{2m-2}$, where C_i is either A_i or B_i with the ‘‘upper’’ block

$$A_i = \begin{cases} [v_2^1, 1], & \text{if } i \text{ is even,} \\ [v_1^1, v_1^3], & \text{if } i \text{ is odd,} \end{cases} \quad (6.7)$$

and the ‘‘lower’’ block

$$B_i = \begin{cases} [-1, v_2^1], & \text{if } i \text{ is even,} \\ [1, v_1^1], & \text{if } i \text{ is odd.} \end{cases} \quad (6.8)$$

By scaling and shifting we can deform each A_i to the interval $[0, 1]$ and B_i to $[-1, 0]$.

Definition 6.7. *We omit the subscript of the sets A_i , B_i and the direct sum \times in the notation. Instead of writing $B_0 \times A_1 \times B_2$ we write BAB . If we want to refer to a face of the cube we will replace the symbol A (B) by the value of the appropriate coordinate, e.g. $B[1]B = \{(x_0, x_1, x_2) \in \mathbb{R}^3 : x_1 \in [-1, 0], x_2 = 1, x_3 \in [-1, 0]\}$. According to Example 6.1 the set $U(1) = B$. Figure 6.3 shows the set $U(2)$ consisting of five cubes*

$$U(2) = BBB \cup BAB \cup AAB \cup BAA \cup AAA.$$

We denote by C^- the union of the faces of the cube C where the intersection number of the free strand \mathbf{u} with the skeletal strands decreases compared to the interior of C , hence

$$U^-(m) = \bigcup_{C \in U(m)} C^-.$$

The set $U(m)$ can be interpreted in two ways: as a collection of $(2m - 1)$ -dimensional cubes, or as a subvariety of \mathbb{R}^{2m-1} (i.e. the union of the cubes). It should be clear from the context which interpretation to use. Similarly, $U^-(m)$ can and will be interpreted both as a collection of $(2m - 2)$ -dimensional faces and as a subvariety of \mathbb{R}^{2m-1} (i.e. the union of the faces). We remark that the analysis in [4] implies that the exit set $U^-(m)$ is the union of $(2m - 2)$ -dimensional faces (hyperplanes). Indeed, any lower dimensional face in $U^-(m)$ must be a subset of a $(2m - 2)$ -dimensional face in $U^-(m)$, since otherwise it would imply a discontinuity of the flow (which is not possible).

It follows from Example 6.1 that $U^-(1) = \emptyset$. The case of $U^-(2)$ is already more complicated. Figure 6.3 shows that

$$U^-(2) = \{(x_0, x_1, x_2) \in U(2) : x_1 = -1 \text{ or } x_1 = 1 \text{ or } x_0 = 1 \text{ or } x_2 = 1\}.$$

The set $U(2)$ is contractible and the set $U^-(2)$ consists of two disjoint contractible pieces. Hence

$$H_k(U^-(2)) = \begin{cases} \mathbb{Z}^2, & \text{if } k = 0, \\ 0, & \text{otherwise.} \end{cases} \quad (6.9)$$

For $m > 2$ we can no longer draw a picture of $U(m)$. Therefore we introduce a schematic representation. The schematic representation of $U(2)$ and $U^-(2)$ is depicted in Figure 6.3. Each bar in schematic representation consists of $2m - 1$ A/B-labeled boxes and stands for a cube with the coordinates given by its label. If the upper (lower) part of the box, in the bar, is shaded then the upper (lower) face of the cube at the corresponding dimension is in $U^-(m)$. For example, Figure 6.3 reveals that the face $B[-1]B \subset U^-(2)$ because the second box of BBB has its lower part shaded. If there is a connecting line between two cubes then they have a common face; the coordinate of the common face is indicated by the position of the end points of the connecting line.

We already mentioned that $U(2)$ consists of five cubes depicted in Figure 6.3. Now we discuss some important properties of the set $U(m)$ for $m \geq 2$. The representative \mathbf{u} used to define the braid class $[\mathbf{u}^I] \text{ rel } \mathbf{w}$ for $I = \{2, \dots, m + 1\}$ is chosen in such a way that its anchor points

u_i with $i \in J_1$ are in the cube $\mathbf{C} = C_0 \cdots C_{2m-2}$ where $C_i = B$ for all i . Hence the cube $BB \cdots B \subset U(m)$. The representative \mathbf{u} , or rather $\beta(\mathbf{u})$, has $2m$ intersections with the strands $\mathbf{v}^1 \cup \mathbf{v}^2$ for $t \in [3, 3 + 2m]$. This number has to be the same for every representative. Since the freedom of movement of coordinate u_i is influenced by its direct neighbors only, we can establish the following two rules for cubes in $U(m)$. Let $\mathbf{C} = C_0 \cdots C_{2m-2} \subset U(m)$ then

$$C_{2i} \text{ can be both A and B} \iff C_{2i-1} \text{ and } C_{2i+1} \text{ are different,} \quad (6.10)$$

while

$$C_{2i+1} \text{ can be both A and B} \iff C_{2i} = B \text{ and } C_{2i+2} = B. \quad (6.11)$$

Starting from the fact that $BB \cdots B \subset U(m)$ we can use these rules to establish that certain configurations are unreachable within $U(m)$, i.e., without leaving the braid class by creating or losing intersections. In particular, since the above rules imply that the following two configurations are “stuck” (none of the letters can change within $U(m)$), they cannot be deformed into $BB \cdots B$ and hence are not in $U(m)$:

Remark 6.8. Let $\mathbf{C} = C_0 \cdots C_{2m-2} \subset U(m)$. Then $C_{2i-1}C_{2i}C_{2i+1}$ cannot be of the form BAB or AAA for any i .

Remark 6.9. From the definition of $U(m)$ we can extend the coding to the “boundary” elements $C_{-1} = C_{2m-1} = B$, which are thus fixed. This observation can be combined with Remark 6.8 to draw conclusions about C_0 and C_{2m-2} for cubes in $U(m)$.

The following lemma shows that the set $U(m)$ is contractible.

Lemma 6.10. The set $U(m)$ is contractible for every $m \in \mathbb{N}$.

Proof. Any cube $C_0, \dots, C_{2m-2} \subset U(m)$ contains the point $(0, \dots, 0)$. For arbitrary $m \in \mathbb{N}$ the set $U(m)$ is star shaped around the point $(0, \dots, 0)$ and can be contracted to this point. Therefore the set $U(m)$ is contractible for every $m \in \mathbb{N}$. ■

The complexity of the set $U^-(m)$ increases with m . See Figure 6.5 for a schematic representation of $U(3)$ and $U^-(3)$. To get a handle on the complexity, and to eventually obtain an inductive description, of $U^-(m)$, we decompose it into two sets $\mathcal{A}_m^-, \mathcal{B}_m^-$, i.e.

$$U^-(m) = \mathcal{A}_m^- \cup \mathcal{B}_m^-.$$

The set \mathcal{A}_m^- is a part of the set $U^-(m)$ which is contained in a union of the cubes $\mathbf{C} = C_0C_1 \cdots C_{2m-2}$ with $C_1 = A$ while the set \mathcal{B}_m^- is a restriction of the set $U^-(m)$ to the cubes with $C_1 = B$. The sets $\mathcal{A}_m^-, \mathcal{B}_m^-$ will turn out to be contractible. Moreover, we will prove that

$$H_*(\mathcal{A}_m^- \cap \mathcal{B}_m^-) = H_*(\mathcal{A}_{m-1}^- \cup \mathcal{B}_{m-1}^-).$$

Then the Mayer-Vietoris sequence makes it possible to compute

$$H_*(U^-(m)) = H_*(\mathcal{A}_m^- \cup \mathcal{B}_m^-)$$

if we know $H_*(\mathcal{A}_{m-1}^- \cup \mathcal{B}_{m-1}^-)$, and by induction we can compute the homology of the set $U^-(m)$ for arbitrary $m \in \mathbb{N}$, see Lemma 6.17.

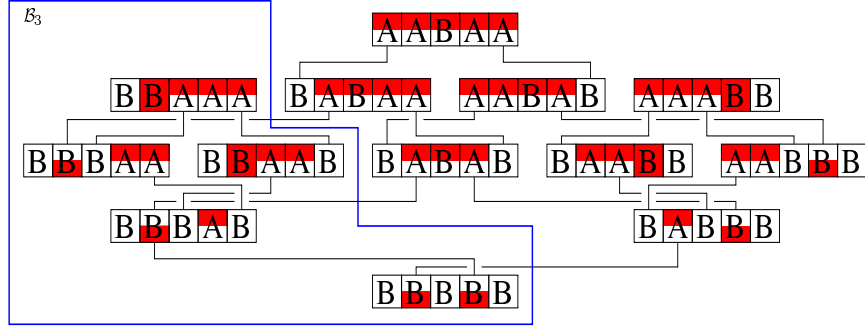


Figure 6.5. Schematic representation of $U(3)$. The shaded faces form $U^-(3)$. The cubes in the polygon form \mathcal{B}_3 and the other cubes form \mathcal{A}_3 .

Definition 6.11. Define

$$\mathcal{A}_m = \bigcup \{C_0 A C_2 \dots C_{2m-2} \subset U(m)\},$$

$$\mathcal{B}_m = \bigcup \{C_0 B C_2 \dots C_{2m-2} \subset U(m)\},$$

and

$$\mathcal{A}_m^- = \bigcup_{\mathbf{C} \subset \mathcal{A}_m} \mathbf{C}^-,$$

$$\mathcal{B}_m^- = \bigcup_{\mathbf{C} \subset \mathcal{B}_m} \mathbf{C}^-.$$

Remark 6.12. For $\mathbf{u} \in [\mathbf{u}^I] \text{ rel } \mathbf{w}$ with $I = \{2, \dots, m+1\}$ the anchor point $u_3 \in [1, v_1^1]$ which corresponds to B , see Figure 6.2. Remark 6.9 implies that $C_0 = B$ for every cube $\mathbf{C} \in \mathcal{B}_m$.

Example 6.13. For the case $m = 2$, the set $\mathcal{B}_2 = \{BBB\}$ and $\mathcal{B}_2^- = \{B[-1]B\}$, while \mathcal{A}_2^- is the rest of the set $U^-(2)$ and \mathcal{A}_2 consists of four remaining cubes, see Figure 6.3. We see that $\mathcal{A}_2^- \cap \mathcal{B}_2^- = \mathcal{A}_1^- \cup \mathcal{B}_1^- = \emptyset$ indeed.

Before we show that \mathcal{A}_m^- and \mathcal{B}_m^- are contractible, we investigate the diagram of $U^-(3)$ in Figure 6.5. For every cube $C_0 A C_2 C_3 C_4 \subset U(3)$ the face $C_0[1]C_2 C_3 C_4 \subset U^-(3)$ and $C_0[0]C_2 C_3 C_4 \not\subset U^-(3)$. By taking into account that the behavior of any anchor point u_i is influenced only by its immediate neighbors u_{i-1} and u_{i+1} , and the fact that all combinations $C_0 A C_2 \dots$ with $C_0, C_2 \in \{A, B\}$ occur already in \mathcal{A}_3 , one can generalize this for any cube $C_0 A C_2 C_3 \dots C_{2m-2} \in \mathcal{A}_m \subset U(m)$ as follows:

$$C_0[1]C_2 C_3 \dots C_{2m-2} \in \mathcal{A}_m^- \subset U^-(m), \quad (6.12)$$

$$C_0[0]C_2 C_3 \dots C_{2m-2} \notin \mathcal{A}_m^- \subset U^-(m). \quad (6.13)$$

Similarly, by inspection of the cubes $B B C_2 C_3 C_4 \subset U(3)$ we conclude that if $B B C_2 C_3 \dots C_{2m-2} \in \mathcal{B}_m \subset U(m)$ then

$$B[-1]C_2 C_3 \dots C_{2m-2} \in \mathcal{B}_m^- \subset U^-(m), \quad (6.14)$$

$$B[0]C_2C_3 \dots C_{2m-2} \in \mathcal{B}_m^- \subset U^-(m) \text{ if and only if } C_2 = A. \quad (6.15)$$

Lemma 6.14. *The sets \mathcal{A}_m^- and \mathcal{B}_m^- are contractible for every $m \in \mathbb{N}$.*

Proof. It follows from (6.13) that $C_0[0]C_2 \dots C_{2m-2} \notin \mathcal{A}_m^-$. On the other hand, $C_0[1]C_2 \dots C_{2m-2} \in \mathcal{A}_m^-$ by (6.12). Hence the map $h : \mathcal{A}_m^- \times [0, 1] \rightarrow \mathcal{A}_m^-$ given by:

$$h(x_0, \dots, x_{2m-2}, t) = (x_0, x_1 + t(1 - x_1), x_2, \dots, x_{2m-2})$$

is a homotopy between the set \mathcal{A}_m^- and

$$\mathcal{A}_m^-|_{x_1=1} := \{\mathbf{x} \in \mathcal{A}_m^- : x_1 = 1\}.$$

We infer from (6.12) that the set $\mathcal{A}_m^-|_{x_1=1}$ is the union of all $(2m-2)$ -dimensional cubes $C_0[1]C_2 \dots C_{2m-2}$ that satisfy $C_0AC_2 \dots C_{2m-2} \subset \mathcal{A}_m^-$. Hence $\mathcal{A}_m^-|_{x_1=1}$ is star shaped with respect to $(0, 1, 0, \dots, 0)$. This implies that \mathcal{A}_m^- is contractible.

Proving contractibility of \mathcal{B}_m^- requires considerably more effort. Decompose \mathcal{B}_m into

$$\mathcal{S} = \bigcup \{\text{BBAC}_3 \dots C_{2m-2} \subset \mathcal{B}_m\},$$

$$\mathcal{T} = \bigcup \{\text{BBBC}_3 \dots C_{2m-2} \subset \mathcal{B}_m\},$$

then

$$\mathcal{B}_m^- = \mathcal{S}^- \cup \mathcal{T}^-,$$

where $\mathcal{S}^- = \{\mathbf{C}^- : \mathbf{C} \subset \mathcal{S}\}$ and $\mathcal{T}^- = \{\mathbf{C}^- : \mathbf{C} \subset \mathcal{T}\}$. For $m \leq 2$ the set $\mathcal{S} = \emptyset$. Note that if $\mathbf{C} = \text{BBAC}_3 \dots C_{2m-2} \subset \mathcal{S}$ then according to Remark 6.8 it holds that $C_3 = A$ and the faces $B[0]AAC_4 \dots C_{2m-2}$ and $\text{BB}[1]AC_4 \dots C_{2m-2}$ are in \mathcal{S}^- , see (6.15) and Figure 6.5 (exploiting one again that only the neighboring boxes C_1 and C_3 determine the boundary behavior at $\text{BB}[1]AC_4 \dots C_{2m-2}$).

One again we use a decomposition, this time of \mathcal{S}^- . Let

$$\mathcal{S}_0^- \stackrel{\text{def}}{=} \bigcup \{B[0]AAC_4 \dots C_{2m-2} \subset \mathcal{S}^-\} = \bigcup \{B[0]AAC_4 \dots C_{2m-2} \mid \text{BBAAC}_4 \dots C_{2m-2} \in \mathcal{S}\},$$

and \mathcal{S}_1^- is the union of all the other $(2m-2)$ -dimensional faces in \mathcal{S}^- . Then we write

$$\mathcal{B}_m^- = \mathcal{S}_0^- \cup (\mathcal{S}_1^- \cup \mathcal{T}^-).$$

The set \mathcal{S}_0^- is a union of $(2m-2)$ -dimensional cubes, which is star shaped around $(0, \dots, 0)$ and hence contractible. For any cube $\mathbf{C} = C_0BC_2 \dots C_{2m-2} \subset \mathcal{B}_m$ it holds that the face $C_0[-1]C_2 \dots C_{2m-2}$ is present in $\mathcal{S}_1^- \cup \mathcal{T}^-$ by (6.14), while $C_0[0]C_2 \dots C_{2m-2}$ is not (combining (6.15) with the definition of the above decomposition of \mathcal{S}^-). The same argument as for \mathcal{A}_m^- furnishes that $\mathcal{S}_1^- \cup \mathcal{T}^-$ is contractible. To show that $\mathcal{B}_m^- = \mathcal{S}_0^- \cup (\mathcal{S}_1^- \cup \mathcal{T}^-)$ is contractible it remains to prove that $\mathcal{S}_0^- \cap (\mathcal{S}_1^- \cup \mathcal{T}^-)$ is contractible.

First, we will prove that

$$\mathcal{S}_0^- \cap (\mathcal{S}_1^- \cup \mathcal{T}^-) = \mathcal{S}_0^- \cap \mathcal{S}_1^-. \quad (6.16)$$

For any cube $\mathbf{C} \in \mathcal{T}$ we have to show that

$$\mathfrak{S}_0^- \cap \mathbf{C}^- \subset \mathfrak{S}_0^- \cap \mathfrak{S}_1^-.$$

We distinguish three different types of cubes in \mathcal{T} : $\text{BBBA} \dots$, $\text{BBBBB} \dots$ and $\text{BBBBA} \dots$. We start with the first type: if

$$\mathbf{C} = \text{BBBAC}_4 \dots C_{2m-2} \subset \mathcal{T}$$

then it follows from (6.10) that $\tilde{\mathbf{C}} = \text{BBAAC}_4 \dots C_{2m-2} \subset \mathfrak{S}$, and we claim that

$$\mathfrak{S}_0^- \cap \mathbf{C}^- \subset \mathfrak{S}_0^- \cap (\mathfrak{S}_1^- \cap \tilde{\mathbf{C}}^-) \subset \mathfrak{S}_0^- \cap \mathfrak{S}_1^-. \quad (6.17)$$

The second inclusion is trivial. To prove the first inclusion we proceed by observing that

$$\mathfrak{S}_0^- \cap \mathbf{C}^- \subset F \stackrel{\text{def}}{=} \text{B}[0][0]AC_4 \dots C_{2m-2}, \quad (6.18)$$

where F is thus a $(2m-3)$ -dimensional face of both \mathbf{C} and $\tilde{\mathbf{C}}$. We claim that

$$\mathbf{C}^- \cap F \subset \tilde{\mathbf{C}}^- \cap \mathfrak{S}_1^-. \quad (6.19)$$

Combining (6.18) and (6.19) then leads to (6.17).

To prove (6.19) we check separately all $(2m-2)$ -dimensional faces in \mathbf{C}^- that have intersection with F . First of all, let $D = \text{BBBA} \dots$ be a face in \mathbf{C} at a coordinate $i \geq 4$. Then the corresponding face $\tilde{D} = \text{BBAA} \dots$ is in $\tilde{\mathbf{C}}$. Using the fact the behavior at a face is only influenced by the two neighboring coordinates, it follows that $D \subset \mathbf{C}^-$ implies that $\tilde{D} \subset \tilde{\mathbf{C}}^-$. Moreover, $\tilde{D} \subset \mathfrak{S}_1^-$ by the definition of the decomposition of \mathfrak{S}^- .

We are left with the faces in coordinates $i = 0, 1, 2, 3$. By counting intersections the following inferences are straightforward. The faces at coordinate $i = 0$ are not in \mathbf{C}^- . Next, at coordinate $i = 1$, the face $\text{B}[0]BA \dots$ is not in \mathbf{C}^- , while the face $\text{B}[-1]BA \dots$ has empty intersection with F . Similarly, at coordinate $i = 2$ the face $\text{BB}[0]A \dots$ is not in \mathbf{C}^- , while the face $\text{BB}[-1]A \dots$ has empty intersection with F . For $i = 3$, the face $\text{BBB}[0] \dots$ is not in \mathbf{C}^- . Finally, the face $\text{BBB}[1] \dots$ is in \mathbf{C}^- and $\text{BBA}[1] \dots$ is in $\tilde{\mathbf{C}}^-$ as well as in \mathfrak{S}_1^- , proving the claim (6.19) for this final face also.

Moving on to the second type of cube in \mathcal{T} , for $\mathbf{C} = \text{BBBBBC}_5 \dots C_{2m-2} \subset \mathcal{T}$ relation (6.17) holds with $\tilde{\mathbf{C}} = \text{BBAABC}_5 \dots C_{2m-2}$, which is in \mathfrak{S} . In this case $\mathfrak{S}_0^- \cap \mathbf{C}^- \subset \text{B}[0][0][0]BC_5 \dots C_{2m-2}$. The faces of \mathbf{C} for $i = 0$ and $i = 4$ are not in \mathbf{C}^- . As before the faces of $\mathfrak{S}_0^- \cap \mathbf{C}^-$ at the coordinates $i > 4$ are contained in $\mathfrak{S}_1^- \cap \tilde{\mathbf{C}}^-$, and the coordinates $i = 1, 2, 3$ are dealt with as above.

Finally, for $m > 3$ there are cubes of the third type in \mathcal{T} , i.e., $\mathbf{C} = \text{BBBBAAC}_6 \dots C_{2m-2} \subset \mathcal{T}$ (where $C_5 = A$ by Remark 6.8). From Remark 6.8 it follows that we may decompose \mathfrak{S} as $\mathfrak{S} = \hat{\mathfrak{S}} \cup \tilde{\mathfrak{S}}$, where

$$\begin{aligned} \hat{\mathfrak{S}} &= \bigcup \{ \text{BBAAB} \dots \subset \mathfrak{S} \}, \\ \tilde{\mathfrak{S}} &= \bigcup \{ \text{BBAAAB} \dots \subset \mathfrak{S} \}. \end{aligned}$$

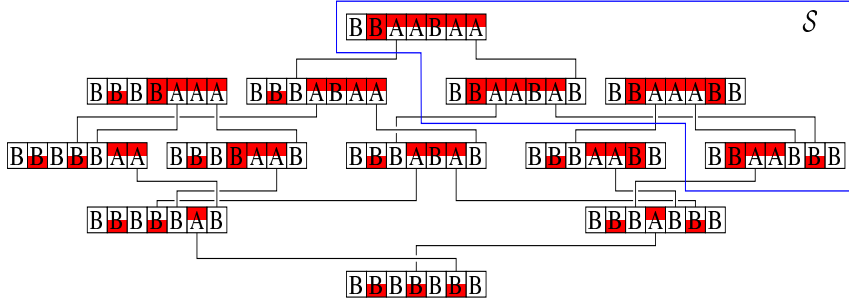


Figure 6.6. Schematic representation of \mathcal{B}_4 . The shaded faces form \mathcal{B}_4^- . The cubes in the polygon form \mathcal{S} and the cubes out of it form \mathcal{T} .

Furthermore, let $\widehat{\mathbf{C}} = \text{BBAABAC}_6 \dots C_{2m-2} \subset \mathcal{S}$. It follows that $\widehat{\mathcal{S}} \cap \mathbf{C} \subset \text{BB}[0][0][0]AC_6, \dots \subset \widehat{\mathbf{C}}^- \cap \mathcal{S}_1^-$ because of the face at coordinate $i = 4$, and we conclude that

$$\mathcal{S}_0^- \cap \mathbf{C}^- \cap \widehat{\mathcal{S}} \subset \mathcal{S}_0^- \cap \mathcal{S}_1^-. \quad (6.20)$$

Next, for any cube $\mathbf{D} \subset \widetilde{\mathcal{S}}$, which can be written as $\mathbf{D} = \text{BBAABD}_6 \dots$, we have that

$$\mathbf{C} \cap \mathbf{D} \subset \text{BB}[0][0]A[0]D_6 \dots \subset \widehat{\mathbf{D}}^- \cap \mathcal{S}_1^-$$

because of the face at coordinate $i = 5$. Hence

$$\mathcal{S}_0^- \cap \mathbf{C}^- \cap \widetilde{\mathcal{S}} \subset \mathcal{S}_0^- \cap \mathcal{S}_1^-. \quad (6.21)$$

From the decomposition of \mathcal{S} and (6.20) and (6.21) we conclude that

$$\mathcal{S}_0^- \cap \mathbf{C} = \mathcal{S}_0^- \cap \mathbf{C} \cap \mathcal{S} \subset \mathcal{S}_0^- \cap \mathcal{S}_1^-.$$

Having thus established the claim (6.16) for the three different types of cubes in \mathcal{T} , to finish the proof of the lemma it is enough to show that $\mathcal{S}_0^- \cap \mathcal{S}_1^-$ is contractible.

If $\mathbf{C} = \text{BBAC}_3 \dots C_{2m-2} \subset \mathcal{S}$ then it follows from Remark 6.8 that $C_3 = A$ and by analyzing the intersection number we obtain that the face $\text{B}[0]AC_3 \dots C_{2m-2} \subset \mathcal{S}_0^-$. All the other faces contained in \mathbf{C}^- belong to \mathcal{S}_1^- . Thus $\mathcal{S}_0^- \cap \mathcal{S}_1^- = \mathcal{S}_1^-|_{x_1=0}$. Moreover for every cube in \mathcal{S} , the face $\text{BB}[1]AC_4 \dots C_{2m-2}$ is in \mathcal{S}_1^- and $\text{BB}[0]AC_4 \dots C_{2m-2}$ is not, see Figure 6.6. Hence $\mathcal{S}_0^- \cap \mathcal{S}_1^- = \mathcal{S}_1^-|_{x_1=0}$ is star shaped around $(0, 0, 1, 0, \dots, 0)$, analogous to the argument at the start of this proof. This implies that the set $\mathcal{S}_0^- \cap \mathcal{S}_1^-$ is contractible. ■

We turn our attention to the set $\mathcal{A}_m^- \cap \mathcal{B}_m^-$. To simplify the arguments we define the sets

$$\begin{aligned} \overline{\mathcal{A}}_m &:= \{\mathbf{C} : \mathbf{C} = \text{AAC}_2 \dots C_{2m-2} \subset \mathcal{A}_m\}, \\ \widetilde{\mathcal{A}}_m &:= \{\mathbf{C} : \mathbf{C} = \text{BAC}_2 \dots C_{2m-2} \subset \mathcal{A}_m\}, \\ \overline{\mathcal{A}}_m^- &:= \{\mathbf{C}^- : \mathbf{C} \in \overline{\mathcal{A}}_m\}, \\ \widetilde{\mathcal{A}}_m^- &:= \{\mathbf{C}^- : \mathbf{C} \in \widetilde{\mathcal{A}}_m\}, \end{aligned}$$

which are all contractible (the proof of contractibility is analogous to the one for \mathcal{A}_m^-). Now $\mathcal{A}_m^- \cup \mathcal{B}_m^- = \overline{\mathcal{A}}_m^- \cup \tilde{\mathcal{A}}_m^- \cup \mathcal{B}_m^-$ and, by arguments similar to those in the proof of Lemma 6.14, $\overline{\mathcal{A}}_m^- \cap (\tilde{\mathcal{A}}_m^- \cup \mathcal{B}_m^-) = \overline{\mathcal{A}}_m^- \cap \tilde{\mathcal{A}}_m^- = \mathcal{A}_m^-|_{x_0=0}$, which is contractible. Therefore

$$H_*(\mathcal{A}_m^- \cup \mathcal{B}_m^-) = H_*(\overline{\mathcal{A}}_m^- \cup \tilde{\mathcal{A}}_m^- \cup \mathcal{B}_m^-) = H_*(\tilde{\mathcal{A}}_m^- \cup \mathcal{B}_m^-). \quad (6.22)$$

Moreover it holds that $\tilde{\mathcal{A}}_m^- \cap \mathcal{B}_m^- = \mathcal{A}_m^- \cap \mathcal{B}_m^-$. Indeed, if $\mathbf{C} = \text{AAC}_2 \dots \text{C}_{2m-2} \subset \mathcal{A}_m$, then $\mathbf{C}^- \cap \mathcal{B}_m^- \subset \widehat{\mathbf{C}}^- \cap \mathcal{B}_m^-$ where $\widehat{\mathbf{C}} = \text{BAC}'_2 \dots \text{C}'_{2m-2}$. Hence we have shown that

$$H_*(\tilde{\mathcal{A}}_m^- \cap \mathcal{B}_m^-) = H_*(\mathcal{A}_m^- \cap \mathcal{B}_m^-). \quad (6.23)$$

Before we start studying the set $\mathcal{A}_m^- \cap \mathcal{B}_m^-$ for arbitrary m , we give a low dimensional example.

Example 6.15. *We claim that*

$$H_*(\mathcal{A}_3^- \cap \mathcal{B}_3^-) = H_*(\mathcal{A}_2^- \cup \mathcal{B}_2^-). \quad (6.24)$$

According to (6.22) and (6.23) it is enough to show that $H_*(\tilde{\mathcal{A}}_3^- \cap \mathcal{B}_3^-) = H_*(\tilde{\mathcal{A}}_2^- \cup \mathcal{B}_2^-)$. To prove this let us decompose the sets $\tilde{\mathcal{A}}_3$ and \mathcal{B}_3 . The set $\tilde{\mathcal{A}}_3 = \mathcal{P}_1 \cup \mathcal{P}_2$ where $\mathcal{P}_1 = \text{BABBB} \cup \text{BABAB} \cup \text{BABAA}$ and $\mathcal{P}_2 = \text{BAABB}$. On the other hand $\mathcal{B}_3 = \mathcal{Q}_1 \cup \mathcal{Q}_2$ where $\mathcal{Q}_1 = \text{BBBBB} \cup \text{BBBAB} \cup \text{BBBAA}$ and $\mathcal{Q}_2 = \text{BBAAB} \cup \text{BBAAA}$. The set \mathcal{P}_i^- (\mathcal{Q}_i^-) is a union of the faces of the cubes $\mathbf{C} \subset \mathcal{P}_i$ (\mathcal{Q}_i) which are in $\tilde{\mathcal{A}}_3^-$ (\mathcal{B}_3^-) and $\tilde{\mathcal{A}}_3^- = \mathcal{P}_1^- \cup \mathcal{P}_2^-$ ($\mathcal{B}_3^- = \mathcal{Q}_1^- \cup \mathcal{Q}_2^-$). Hence

$$\tilde{\mathcal{A}}_3^- \cap \mathcal{B}_3^- = \bigcup_{i,j=1}^2 \mathcal{P}_i^- \cap \mathcal{Q}_j^-.$$

Careful inspection of Figure 6.5 reveals that $\mathcal{P}_1^- \cap \mathcal{Q}_1^- = \text{B}[0]\text{B}[-1]\text{B} \cup \text{B}[0]\text{B}[1]\text{B} \cup \text{B}[0]\text{B}[1]\text{A} \cup \text{B}[0]\text{BA}[1]$. This is homotopic to the set $0 \times 0 \times \{\text{B}[-1]\text{B} \cup \text{B}[1]\text{B} \cup \text{B}[1]\text{A} \cup \text{BA}[1]\}$, which can be written as $0 \times 0 \times \{\tilde{\mathcal{A}}_2^- \cup \mathcal{B}_2^-\}$, see Figure 6.7. Therefore

$$H_*(\mathcal{P}_1^- \cap \mathcal{Q}_1^-) = H_*(\tilde{\mathcal{A}}_2^- \cup \mathcal{B}_2^-).$$

After a short computation we find

$$\begin{aligned} \mathcal{P}_2^- \cap \mathcal{Q}_1^- &= \text{B}[0][0][-1]\text{B} \subset \mathcal{P}_1^- \cap \mathcal{Q}_1^-, \\ \mathcal{P}_1^- \cap \mathcal{Q}_2^- &= \text{B}[0][0]\text{AB} \cup \text{B}[0][0]\text{AA}, \\ \mathcal{P}_2^- \cap \mathcal{Q}_2^- &= \text{B}[0]\text{A}[0]\text{B}. \end{aligned}$$

The set $(\mathcal{P}_1^- \cap \mathcal{Q}_2^-) \cup (\mathcal{P}_2^- \cap \mathcal{Q}_2^-)$ is contractible, and its intersection with $\mathcal{P}_1^- \cap \mathcal{Q}_1^-$ is given by $\text{B}[0][0][1]\text{B} \cup \text{B}[0][0][1]\text{A} \cup \text{B}[0][0]\text{A}[1]$, which is again contractible. Hence $\tilde{\mathcal{A}}_3^- \cap \mathcal{B}_3^-$ is homotopic to $\mathcal{P}_1^- \cap \mathcal{Q}_1^-$ and

$$H_*(\tilde{\mathcal{A}}_3^- \cap \mathcal{B}_3^-) = H_*(\mathcal{P}_1^- \cap \mathcal{Q}_1^-) = H_*(\tilde{\mathcal{A}}_2^- \cup \mathcal{B}_2^-).$$

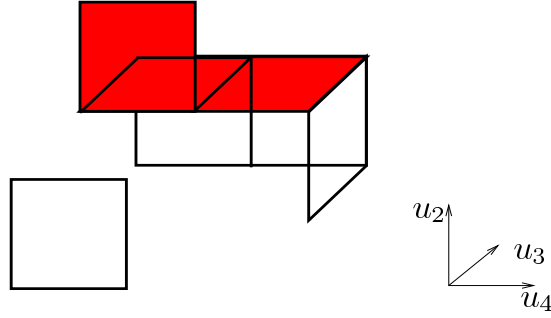


Figure 6.7. The projection of the set $\mathcal{A}_3^- \cap \mathcal{B}_3^-$ on the coordinates (u_2, u_3, u_4) . The unshaded squares form the set $\mathcal{P}_1^- \cap \mathcal{Q}_1^-$.

Lemma 6.16. Let $m \in \mathbb{N}$ such that $m > 1$. Then

$$H_*(\mathcal{A}_m^- \cap \mathcal{B}_m^-) = H_*(\mathcal{A}_{m-1}^- \cup \mathcal{B}_{m-1}^-). \quad (6.25)$$

Proof. According to (6.23) it holds that

$$H_*(\mathcal{A}_m^- \cap \mathcal{B}_m^-) = H_*(\tilde{\mathcal{A}}_m^- \cap \mathcal{B}_m^-).$$

Every cube $\mathbf{C} = C_0 C_1 \dots C_{2m-2} \subset \tilde{\mathcal{A}}_m^- \cup \mathcal{B}_m^-$ satisfies that $C_0 = B$, and the two faces $[-1]C_1 \dots C_{2m-2}$ and $[0]C_1 \dots C_{2m-2}$ are not present in $\tilde{\mathcal{A}}_m^- \cup \mathcal{B}_m^-$. By homotopy invariance, this implies that $H_*(\tilde{\mathcal{A}}_m^- \cap \mathcal{B}_m^-) = H_*(\tilde{\mathcal{A}}_m^-|_{x_0=0} \cap \mathcal{B}_m^-|_{x_0=0})$, where $\tilde{\mathcal{A}}_m^-|_{x_0=0} = \{\mathbf{x} \in \tilde{\mathcal{A}}_m^- : x_0 = 0\}$ and $\mathcal{B}_m^-|_{x_0=0} = \{\mathbf{x} \in \mathcal{B}_m^- : x_0 = 0\}$. In order to evaluate $H_*(\tilde{\mathcal{A}}_m^-|_{x_0=0} \cap \mathcal{B}_m^-|_{x_0=0})$ we decompose $\tilde{\mathcal{A}}_m^-|_{x_0=0}$ and $\mathcal{B}_m^-|_{x_0=0}$ as follows:

$$\mathcal{P}_1 = \bigcup \{\mathbf{C} \in \tilde{\mathcal{A}}_m^-|_{x_0=0} : C_2 = B\}, \quad \mathcal{P}_2 = \bigcup \{\mathbf{C} \in \tilde{\mathcal{A}}_m^-|_{x_0=0} : C_2 = A\},$$

$$\mathcal{Q}_1 = \bigcup \{\mathbf{C} \in \mathcal{B}_m^-|_{x_0=0} : C_2 = B\}, \quad \mathcal{Q}_2 = \bigcup \{\mathbf{C} \in \mathcal{B}_m^-|_{x_0=0} : C_2 = A\}.$$

The set \mathcal{P}_i^- (\mathcal{Q}_i^-) is the union of the faces of the $(2m-2)$ -dimensional cubes $\mathbf{C} = [0]C_1 \dots C_{2m-2} \subset \mathcal{P}_i^-$ (\mathcal{Q}_i^-), which are in $\tilde{\mathcal{A}}_m^-|_{x_0=0}$ ($\mathcal{B}_m^-|_{x_0=0}$). According to Remark 6.8, if $\mathbf{C} \subset \mathcal{P}_2$ then $C_3 = B$, while if $\mathbf{C} \subset \mathcal{Q}_2$ then $C_3 = A$. We decompose the intersection

$$\tilde{\mathcal{A}}_m^-|_{x_0=0} \cap \mathcal{B}_m^-|_{x_0=0} = \bigcup_{i,j=1}^2 (\mathcal{P}_i^- \cap \mathcal{Q}_j^-).$$

It holds that $\mathcal{P}_1 \cap \mathcal{Q}_1 \subset [0][0]BC_3 \dots C_{2m-2}$. For any cube $\mathbf{C} = [0]C_1 C_2 \dots C_{2m-2} \subset \mathcal{P}_1$ it holds that $C_1 = A$ and $C_2 = B$, hence $[0][0]C_2 \dots C_{2m-2} \notin \mathcal{P}_1^-$ and $[0]C_1[-1]C_3 \dots C_{2m-2} \notin \mathcal{P}_1^-$. Moreover, for any cube $\mathbf{C} = [0]C_1 C_2 \dots C_{2m-2} \subset \mathcal{Q}_1$ it holds that $C_1 = B$ and $C_2 = B$, hence $[0]C_1[0]C_3 \dots C_{2m-2} \notin \mathcal{Q}_1^-$. We conclude that the intersections of \mathcal{P}_1^- and \mathcal{Q}_1^- are due to

faces with coordinates $i \geq 3$. The fact that $C_2 = B$ for every cube in \mathcal{P}_1 and \mathcal{Q}_1 now implies that $(\mathcal{P}_1^- \cap \mathcal{Q}_1^-) = 0 \times 0 \times (\tilde{\mathcal{A}}_{m-1}^- \cup \mathcal{B}_{m-1}^-)$. Hence

$$H_*(\mathcal{P}_1^- \cap \mathcal{Q}_1^-) = H_*(\tilde{\mathcal{A}}_{m-1}^- \cup \mathcal{B}_{m-1}^-) = H_*(\mathcal{A}_{m-1}^- \cup \mathcal{B}_{m-1}^-),$$

where we have used (6.22).

If $\mathbf{C} \subset \mathcal{P}_2 \cap \mathcal{Q}_1$ then

$$\mathbf{C} = [0][0][0]BC_4 \dots C_{2m-2} \subset [0][0]BBC_4 \dots C_{2m-2} \subset \mathcal{P}_1 \cap \mathcal{Q}_1.$$

Non of the faces for $i = 0, 1, 2$ is in $\mathcal{P}_2^- \cap \mathcal{Q}_1^-$. Hence $\mathcal{P}_2^- \cap \mathcal{Q}_1^- \subset \mathcal{P}_1^- \cap \mathcal{Q}_1^-$, and $H_*((\mathcal{P}_1^- \cap \mathcal{Q}_1^-) \cup (\mathcal{P}_2^- \cap \mathcal{Q}_1^-)) = H_*(\mathcal{P}_1^- \cap \mathcal{Q}_1^-)$. To prove the relation

$$H_*(\tilde{\mathcal{A}}_m^-|_{x_0=0} \cap \mathcal{B}_m^-|_{x_0=0}) = H_*(\mathcal{P}_1^- \cap \mathcal{Q}_1^-) = H_*(\mathcal{A}_{m-1}^- \cup \mathcal{B}_{m-1}^-), \quad (6.26)$$

it is enough to show that

$$V := (\mathcal{P}_1^- \cap \mathcal{Q}_2^-) \cup (\mathcal{P}_2^- \cap \mathcal{Q}_2^-) \quad (6.27)$$

is contractible and that its intersection with $\mathcal{P}_1^- \cap \mathcal{Q}_1^-$ is contractible. We prove that V is contractible by showing that both components in (6.27) are contractible and so is their intersection.

The set \mathcal{P}_1 is built up from cubes of the form $[0]ABC_3 \dots C_{2m-2}$, while cubes in \mathcal{Q}_2 have the form $[0]BAAC_4 \dots C_{2m-2}$. The cube $[0]ABAC_4 \dots C_{2m-2}$ is in \mathcal{P}_1 if and only if $[0]BAAC_4 \dots C_{2m-2}$ is in \mathcal{Q}_2 . Moreover, any $(2m-4)$ -dimensional face $[0][0][0]AC_4 \dots C_{2m-2}$ is in $\mathcal{P}_1^- \cap \mathcal{Q}_2^-$. Therefore $\mathcal{P}_1^- \cap \mathcal{Q}_2^-$ is the union of the $(2m-4)$ -dimensional cubes $[0][0][0]AC_4 \dots C_{2m-2}$ that are in \mathcal{Q}_2 , which is star shaped around $(0, \dots, 0)$. This implies that $\mathcal{P}_1^- \cap \mathcal{Q}_2^-$ is contractible.

If $\hat{\mathbf{C}} \subset \mathcal{P}_2 \cap \mathcal{Q}_2$ then $\hat{\mathbf{C}} = [0][0]A[0]C_4 \dots C_{2m-2} \subset \mathcal{P}_2$. Moreover, for any cube in $\mathbf{C} = C_1C_2 \dots C_{2m-2}$ in \mathcal{P} , we have that $\hat{\mathbf{C}} = [0][0]A[0]C_4 \dots C_{2m-2} \subset \mathcal{P}_2^-$ because of the face at $i = 3$. On the other hand, for any cube in $\mathbf{D} = D_1D_2 \dots D_{2m-2}$ in \mathcal{Q} , we have that $\hat{\mathbf{D}} = [0][0]A[0]D_4 \dots D_{2m-2} \subset \mathcal{Q}_2^-$ because of the face at $i = 1$. Therefore the set $\mathcal{P}_2^- \cap \mathcal{Q}_2^-$ is the union of the intersections of the \mathbf{C} and \mathbf{D} :

$$\mathcal{P}_2^- \cap \mathcal{Q}_2^- = \bigcup \{\hat{\mathbf{C}} \cap \hat{\mathbf{D}} \mid \mathbf{C} \in \mathcal{P}_2, \mathbf{D} \in \mathcal{Q}_2\}.$$

Since the origin is in all of the intersections, their union, $\mathcal{P}_2^- \cap \mathcal{Q}_2^-$, is star shaped and contractible.

We now consider the intersection $(\mathcal{P}_1^- \cap \mathcal{Q}_2^-) \cap (\mathcal{P}_2^- \cap \mathcal{Q}_2^-) = \mathcal{P}_1^- \cap \mathcal{P}_2^- \cap \mathcal{Q}_2^-$. When a face \mathbf{C} is in $\mathcal{P}_1 \cap \mathcal{P}_2 \cap \mathcal{Q}_2$, then \mathbf{C} is contained in a $(2m-5)$ -dimensional face of the form $[0][0][0][0]C_4 \dots C_{2m-2}$. Hence it follows from the arguments above that any face in $\mathcal{P}_1 \cap \mathcal{P}_2 \cap \mathcal{Q}_2$ is contained in $\mathcal{P}_1^- \cap \mathcal{P}_2^- \cap \mathcal{Q}_2^-$. As before, this implies that $\mathcal{P}_1^- \cap \mathcal{P}_2^- \cap \mathcal{Q}_2^-$ is a union of intersections of cubes, and it is thus star shaped with respect to the origin.

We have proved that the sets $\mathcal{P}_1^- \cap \mathcal{Q}_2^-$ and $\mathcal{P}_2^- \cap \mathcal{Q}_2^-$ are contractible, as well as their intersection. We thus infer that their union V is contractible.

Finally, any face in the set

$$(\mathcal{P}_1^- \cap \mathcal{Q}_1^-) \cap V = \mathcal{P}_1^- \cap \mathcal{Q}_1^- \cap \mathcal{Q}_2^-$$

is contained in a $(2m-4)$ -dimensional cubes of the form $[0][0][0]AC_4 \cdots C_{2m-2}$. We note that any $(2m-2)$ -dimensional face $[0]ABAC_4 \cdots C_{2m-2}$ is in \mathcal{P}_1 if and only if $[0]BBAC_4 \cdots C_{2m-2}$ is in \mathcal{Q}_1 if and only if $[0]ABAC_4 \cdots C_{2m-2}$ is in \mathcal{Q}_2 . As discussed above, for any $[0]ABAC_4 \cdots C_{2m-2}$ in \mathcal{Q}_2 , the $(2m-4)$ -dimensional face $[0][0][0]AC_4 \cdots C_{2m-2}$ is in $\mathcal{P}_1^- \cap \mathcal{Q}_2^-$. Furthermore, the $(2m-5)$ -dimensional face $[0][0][0][1]C_4 \cdots C_{2m-2}$ is contained in \mathcal{Q}_1^- for any $[0]ABAC_4 \cdots C_{2m-2} \in \mathcal{Q}_2$, whereas $[0][0][0][0]C_4 \cdots C_{2m-2}$ is not in \mathcal{Q}_1^- . A homotopy analogous to the one in the proof of Lemma 6.14 shows that the set $(\mathcal{P}_1^- \cap \mathcal{Q}_1^-) \cap V$ is contractible. This proves the relation (6.26).

■

The following lemma describes the homology of the set $U^-(m)$ for arbitrary $m \in \mathbb{N}$.

Lemma 6.17. *The homology of the set $U^-(m)$, for $m > 0$, is given by*

$$H_k(U^-(m)) = H_k(\Gamma^{m-1}) = \begin{cases} \mathbb{Z} & k = 0, m - 2, \\ 0 & \text{otherwise.} \end{cases}$$

where Γ^n is the boundary of the n -dimensional unit cube $[0, 1]^n$.

Remark 6.18. *We use the convention $H_k(\Gamma^0) = 0$ for $k \in \mathbb{Z}$.*

Proof. At the beginning of this subsection we proved the lemma for $m = 1, 2$. We use induction to prove the lemma for arbitrary m , the induction hypothesis being that $H_k(U^-(m-1)) = H_k(\Gamma^{m-2})$. We now consider $U^-(m) = \mathcal{A}_m^- \cup \mathcal{B}_m^-$. According to Lemma 6.14 the sets \mathcal{A}_m^- and \mathcal{B}_m^- are contractible. Lemma 6.16 furnishes

$$H_*(\mathcal{A}_m^- \cap \mathcal{B}_m^-) = H_*(\mathcal{A}_{m-1}^- \cup \mathcal{B}_{m-1}^-),$$

hence the induction hypothesis implies that

$$H_*(\mathcal{A}_m^- \cap \mathcal{B}_m^-) = H_*(\Gamma^{m-2}).$$

By exploiting the exactness of the Mayer-Vietoris sequence (see e.g. [5])

$$\dots \xrightarrow{\varphi_k^*} H_k(\mathcal{A}_m^-) \oplus H_k(\mathcal{B}_m^-) \xrightarrow{\psi_k^*} H_k(\mathcal{A}_m^- \cup \mathcal{B}_m^-) \xrightarrow{\partial_k^*} H_{k-1}(\mathcal{A}_m^- \cap \mathcal{B}_m^-) \xrightarrow{\varphi_{k-1}^*} H_{k-1}(\mathcal{A}_m^-) \oplus H_{k-1}(\mathcal{B}_m^-) \xrightarrow{\psi_{k-1}^*} \dots$$

and using Lemma 6.14, we conclude that $H_*(\mathcal{A}_m^- \cup \mathcal{B}_m^-) = H_*(\Gamma^{m-1})$. ■

6.5. The computation of $H_*(\mathbf{H}(\mathbf{u}^I \# \mathbf{w}, 2p))$. Having done the hard work in §6.4, we now put the pieces together. First we recall that the sets N_I and N_I^- decompose as follows

$$N_I = U_0 \times U_1 \times \dots \times U_l,$$

$$N_I^- = \bigcup_{i=0}^l U_0 \times U_1 \times \dots \times U_{i-1} \times U_i^- \times U_{i+1} \times \dots \times U_l.$$

The homology of the sets U_0 and U_0^- is given by (6.5) and (6.6). The homology of U_i and U_i^- is computed in Lemma 6.10 and Lemma 6.17. We use them to compute $H_*(N_I)$ and $H_*(N_I^-)$. Then by using the exact sequence which relates $H_*(N_I)$, $H_*(N_I^-)$ to $H_*(N_I, N_I^-)$ we calculate $H_*(\mathbf{H}(\mathbf{u}^I \# \mathbf{w}, 2p)) = H_*(N_I, N_I^-)$.

Lemma 6.19. *The set N_I is contractible, whereas the homology of N_I^- is given by*

$$H_k(N_I^-) = \begin{cases} \mathbb{Z}, & \text{if } k = 0, 2p - \#I - 1, \\ 0, & \text{otherwise.} \end{cases} \quad (6.28)$$

Proof. The set N_I is a direct sum of the contractible sets U_i . Hence it is contractible. It remains to prove that homology of N_I^- is given by (6.28). We start by computing the homology of the union

$$U_0^- \times U_1 \times U_2 \times \dots \times U_l \cup U_0 \times U_1^- \times U_2 \times \dots \times U_l.$$

Since the sets U_i are contractible,

$$H_*(U_0^- \times U_1 \times U_2 \times \dots \times U_l \cup U_0 \times U_1^- \times U_2 \times \dots \times U_l) = H_*(U_0^- \times U_1 \cup U_0 \times U_1^-),$$

and

$$\begin{aligned} H_*(U_0^- \times U_1) &= H_*(U_0^-) = H_*(\Gamma^M), \\ H_*(U_0 \times U_1^-) &= H_*(U_1^-) = H_*(\Gamma^N), \end{aligned}$$

where Γ^M is the boundary of an M dimensional cube and $M = \#\mathcal{J}_0$, while $N = (\#\mathcal{J}_1 - 1)/2$.

To guide our thoughts, suppose for a moment that \tilde{U}_0 is an M -dimensional cube and $\tilde{U}_0^- = \partial\tilde{U}_0$, while $\tilde{U}_1^- = \partial\tilde{U}_1$ and \tilde{U}_1 is an N -dimensional cube. Then

$$\partial(\tilde{U}_0 \times \tilde{U}_1) = \partial\tilde{U}_0 \times \tilde{U}_1 \cup \tilde{U}_0 \times \partial\tilde{U}_1 = \tilde{U}_0^- \times \tilde{U}_1 \cup \tilde{U}_0 \times \tilde{U}_1^-,$$

and

$$H_*(\tilde{U}_0^- \times \tilde{U}_1 \cup \tilde{U}_0 \times \tilde{U}_1^-) = H_*(\partial(\tilde{U}_0 \times \tilde{U}_1)) = H_*(\Gamma^{M+N}).$$

However, this is too much of a simplification, since in our case it only holds that $U_i^- \subset U_i$, where U_i is contractible and $H_*(U_0^-) = H_*(\Gamma^M)$ while $H_*(U_1^-) = H_*(\Gamma^N)$. Nevertheless, we still claim that

$$H_*(U_0^- \times U_1 \cup U_0 \times U_1^-) = H_*(\Gamma^{M+N}). \quad (6.29)$$

If $M = 0$ or $N = 0$ then $U_0^- = \emptyset$, or $U_1^- = \emptyset$ and (6.29) is trivially satisfied. For M and N both positive we use the long exact sequence

$$\dots \xrightarrow{\partial_{k+1}^*} H_k(A \cap B) \xrightarrow{\varphi_k^*} H_k(A) \oplus H_k(B) \xrightarrow{\psi_k^*} H_k(A \cup B) \xrightarrow{\partial_k^*} H_{k-1}(A \cap B) \xrightarrow{\varphi_{k-1}^*} \dots \quad (6.30)$$

to prove (6.29). Let $A = U_0^- \times U_1$ and $B = U_0 \times U_1^-$, then

$$A \cap B = U_0^- \times U_1^-.$$

Without the loss of generality we can suppose that $M \geq N$. The homology

$$H_*(A \cap B) = H_*(U_0^- \times U_1^-) = H_*(\Gamma^M \times \Gamma^N)$$

is the homology of the cross product of two spheres, i.e., only the homology groups 0 , $M - 1$, $N - 1$ and $M + N - 2$ are nontrivial. If these four indices are all different, then the nontrivial

groups are \mathbb{Z} . In case some of the indexes are the same then the group is \mathbb{Z}^k , where k is the number of the indices that refer to this group. When we plug the known homologies $H_*(A)$, $H_*(B)$ and $H_*(A \cap B)$ into the exact sequence (6.30), we see that we need to distinguish six cases: $M = N = 1$, $M - 1 = N = 1$, $M - 1 > N = 1$, $M = N > 1$, $M - 1 = N > 1$ and $M - 1 > N > 1$. We will deal with the case $M - 1 > N > 1$ only. All the other cases can be treated analogously. In this case

$$H_k(A) = \begin{cases} \mathbb{Z}, & \text{if } k = 0, M - 1, \\ 0, & \text{otherwise,} \end{cases} \quad H_k(B) = \begin{cases} \mathbb{Z}, & \text{if } k = 0, N - 1, \\ 0, & \text{otherwise,} \end{cases}$$

$$H_k(A \cap B) = \begin{cases} \mathbb{Z}, & \text{if } k = 0, N - 1, M - 1, M + N - 2, \\ 0, & \text{otherwise.} \end{cases}$$

The homology group $H_{M+N-1}(A \cup B) = \mathbb{Z}$ because of the short exact sequence

$$0 \xrightarrow{\psi_{M+N-1}^*} H_{M+N-1}(A \cup B) \xrightarrow{\partial_{M+N-1}^*} \mathbb{Z} \xrightarrow{\varphi_{M+N-2}^*} 0,$$

which is a part of the long exact sequence (6.30). Combining the part

$$0 \xrightarrow{\partial_M^*} \mathbb{Z} \xrightarrow{\varphi_{M-1}^*} \mathbb{Z} \xrightarrow{\psi_{M-1}^*} H_{M-1}(A \cup B) \xrightarrow{\partial_{M-1}^*} 0,$$

with the fact that $\text{im} \varphi_{M-1}^* = \mathbb{Z}$ (since $H_{M-1}(B) = 0$) implies that $H_{M-1}(A \cup B) = 0$. Similar calculations provide that $H_{N-1}(A \cup B) = 0$. Finally, by exploiting the exact sequence

$$0 \xrightarrow{\psi_1^*} H_1(A \cup B) \xrightarrow{\partial_1^*} \mathbb{Z} \xrightarrow{\varphi_0^*} \mathbb{Z} \times \mathbb{Z} \xrightarrow{\psi_0^*} H_0(A \cup B) \xrightarrow{\partial_0^*} 0,$$

where $\text{im} \varphi_0^* = \mathbb{Z} \times \{0\}$ and $\ker \varphi_0^* = 0$, we obtain that $H_1(A \cup B) = 0$ and $H_0(A \cup B) = \mathbb{Z}$. For all remaining indices the exactness of

$$0 \xrightarrow{\psi_k^*} H_k(A \cup B) \xrightarrow{\partial_k^*} 0,$$

implies that $H_k(A \cup B) = 0$.

We have thus proved the claim (6.29) and we deduce that

$$H_*(U_0^- \times U_1 \times U_2 \times \dots \times U_l \cup U_0 \times U_1^- \times U_2 \times \dots \times U_l) = H_*(\Gamma^{M+N}).$$

By repeating the previous computation l times we obtain that

$$H_*(N_I^-) = H_* \left(\Gamma^{\{\#J_0 + \sum_{i=1}^l (\#J_i - 1)/2\}} \right).$$

According to Definition 6.4 it holds that $\#J_0 = 2p - \sum_{i=1}^l \#J_i$ and $\#I = \sum_{i=1}^l (\#J_i + 1)/2$, hence

$$H_k(N_I^-) = H_k \left(\Gamma^{\{2p - \#I\}} \right) = \begin{cases} \mathbb{Z}, & \text{if } k = 0, 2p - \#I - 1, \\ 0, & \text{otherwise.} \end{cases}$$

■

To conclude the proof of Theorem 5.3, we compute the relative homology $H_*(N_I, N_I^-)$. We use the long exact sequence for the pair (N_I, N_I^-) :

$$\dots \xrightarrow{\partial_{k+1}^*} H_k(N_I^-) \xrightarrow{i_k^*} H_k(N_I) \xrightarrow{\pi_k^*} H_k(N_I, N_I^-) \xrightarrow{\partial_k^*} H_{k-1}(N_I^-) \xrightarrow{i_{k-1}^*} \dots$$

For $k \notin \{0, 2p - \#I\}$ exactness of

$$0 \xrightarrow{\pi_k^*} H_k(N_I, N_I^-) \xrightarrow{\partial_k^*} 0$$

implies that $H_k(N_I, N_I^-) = 0$. The exact sequences

$$0 \xrightarrow{\pi_{2p-\#I}^*} H_{2p-\#I}(N_I, N_I^-) \xrightarrow{\partial_{2p-\#I}^*} \mathbb{Z} \xrightarrow{i_{2p-\#I-1}^*} 0,$$

and

$$0 \xrightarrow{\pi_1^*} H_1(N_I, N_I^-) \xrightarrow{\partial_1^*} \mathbb{Z} \xrightarrow{i_0^*} \mathbb{Z} \xrightarrow{\pi_0^*} H_0(N_I, N_I^-) \xrightarrow{\partial_0^*} 0,$$

furnish (since $\ker i_0^* = 0$, $\text{im } i_0^* = \mathbb{Z}$)

$$H_k(N_I, N_I^-) = \begin{cases} \mathbb{Z}, & \text{if } k = 2p - \#I, \\ 0, & \text{otherwise,} \end{cases}$$

which concludes the proof of Theorem 5.3.

7. Forcing of solutions in $[\sigma_1^2 \sigma_2^{2q}, 2p]$. In this section we establish the ordering relation $[\sigma_1^2 \sigma_2^4, 4] \prec [\sigma_1^2 \sigma_2^{2q}, 2p]$, for $3 < q < p$ and estimate the number of geometrically distinct solutions in the class $[\sigma_1^2 \sigma_2^{2q}, 2p]$. To do so we define a braid class $[\mathbf{u}^I]_{\mathcal{E}} \text{ rel } \mathbf{w}$, for every set $I = \{j_1, \dots, j_n\} \subset \mathbb{N}^n$ satisfying

$$p - q + 3 < j_1 < \dots < j_n < p - 1, \quad (7.1)$$

with only $3 < q < p$ required in the special case $I = \emptyset$. As in Section 5 we construct a subset $M_{I,\epsilon}$ of $[\mathbf{u}^I]_{\mathcal{E}} \text{ rel } \mathbf{w}$ which is an isolating neighborhood of the flow Ψ^t generated by the parabolic recurrence relation corresponding to Equation (1.1). As before, the Conley index of $M_{I,\epsilon}$ is given by the invariant $H_*(\mathbf{H}(\mathbf{u}^I \# \mathbf{w}, \mathcal{E}; 2p))$, and non-triviality of the index implies the existence of a fixed point \mathbf{u} of the flow Ψ^t in the set $M_{I,\epsilon}$, which corresponds to a solution $u \in [\sigma_1^2 \sigma_2^{2q}, p]$. Solutions obtained for different sets I are geometrically distinct.

Definition 7.1. Let the skeleton \mathbf{w} be given by (5.3). The braid class $[\mathbf{u}^I]_{\mathcal{E}} \text{ rel } \mathbf{w} \in \mathcal{E}_{2p}^1 \text{ rel } \mathbf{w}$ is defined by its representative \mathbf{u}^I satisfying:

1. $u_0^I \in (v_0^1, v_0^6)$,
2. $u_{2i+1}^I \in \begin{cases} (v_1^4, v_1^5) & : \text{ if } 1 < i < 2 + p - q, \\ (v_1^5, v_1^1) & : \text{ otherwise,} \end{cases}$
3. $u_{2i}^I \in \begin{cases} (v_2^4, v_2^1) & : \text{ if } i \in I \text{ or } 1 < i < 3 + p - q, \\ (v_2^1, v_2^3) & : \text{ otherwise.} \end{cases}$

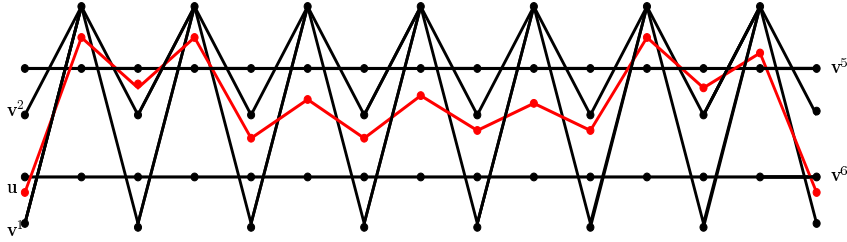


Figure 7.1. A representative of the braid class $[\mathbf{u} \text{ rel } \mathbf{w}]_I \in \mathcal{E}_{14}^1 \text{ rel } \mathbf{w}$ for $q = 4$ and $I = \emptyset$. We did not depict \mathbf{v}^3 , nor \mathbf{v}^4 .

The free strand \mathbf{u} intersects the strand \mathbf{v}^5 four times then it stays below this strand until the anchor point $u_{4+2(p-q)}$. Then it intersects the strand \mathbf{v}^5 four times again. After this the free strand \mathbf{u} behaves in the same way as the free strand of the braid class from the previous section, having fingers at coordinates $i = 2j_k$. Figure 7.1 shows the braid class $[\mathbf{u}^I]_{\mathcal{E}} \text{ rel } \mathbf{w}$ with a simplified skeleton for $q = 3$ and $I = \emptyset$. The procedure for simplifying the skeleton is explained in the previous section.

For the sake of simplicity we restrict ourselves to the case $I = \emptyset$ here. However, the same decomposition of the set of anchor points u_i with $i \in \{4 + 2(p - q), \dots, 2p\}$ as in Sections 5 and 6 extends the result for nonempty sets I . For the remainder of this section we omit I from the notation.

In order to construct an isolating neighborhood which contains a fixed point corresponding to $u \in [\sigma_1^2 \sigma_2^{2q}, 2p]$ with $q < p$ we have to guarantee that anchor points $u_{2i+1} < 1$ for $i = 2, 3, \dots, 1 + p - q$. Before we define the isolating neighborhood let us recall an important property of the parabolic recurrence relation \mathcal{R} generated by (1.1) at the zero energy level. In the parameter range $\alpha \in [0, \sqrt{8})$ the two equilibria $u_{\pm} = \pm 1$ are saddle-foci and there are no solutions which converge monotonically to any of these equilibria. Therefore the twist property, see Section 2, implies that for every $(x, y) \in \mathbb{R}^2 \setminus \Delta$ there exists a finite $\tau_{x,y}$ and a unique solution $u(t; x, y) : [0, \tau_{x,y}] \rightarrow \mathbb{R}$ such that $u(0; x, y) = x$, $u(\tau_{x,y}; x, y) = y$ and $u'|_{(0, \tau_{x,y})} > 0$ if $x < y$ (while $u'|_{(0, \tau_{x,y})} < 0$ if $x > y$). The function \mathcal{R}_i satisfies, see [14],

$$\mathcal{R}_i(u_{i-1}, u_i, u_{i+1}) = u'''(0; u_i, u_{i+1}) - u'''(\tau_{u_{i-1}, u_i}; u_{i-1}, u_i).$$

Finally we investigate the function \mathcal{R}_i for u_i close to $u_+ = 1$. We restrict to odd index i and take $u_{i\pm 1} < u_i = 1$. The fact that $\tau_{u_{i-1}, 1}$ and $\tau_{1, u_{i+1}}$ are always finite combined with Lemma 2.2 in [7] ensures that $u'(\tau_{u_{i-1}, 1}; u_{i-1}, 1) = u''(\tau_{u_{i-1}, 1}; u_{i-1}, 1) = 0$ and $u'''(\tau_{u_{i-1}, 1}; u_{i-1}, 1) \neq 0$. Monotonicity of $u(t; u_{i-1}, 1)$ implies that $u'''(\tau_{u_{i-1}, 1}; u_{i-1}, 1) > 0$. Analogously, $u'''(\tau_{1, u_{i+1}}; 1, u_{i+1}) < 0$ and $\mathcal{R}_i(u_{i-1}, 1, u_{i+1}) > 0$. Due to the uniqueness of the monotone loops (solutions $u(t, x, y)$) the function \mathcal{R}_i is continuous on Ω_i and for sufficiently small $\eta > 0$ it holds that

$$\mathcal{R}_i(u_{i-1}, 1 - \eta, u_{i+1}) < 0.$$

Definition 7.2. Define, with \mathbf{u}^I satisfying Definition 7.1,

$$N_{\delta} = \{\mathbf{u} \in \text{cl}([\mathbf{u}^I]_{\mathcal{E}} \text{ rel } \mathbf{w}) : (-1)^i (u_{i+1} - u_i) \geq \delta\}$$

and let $M_{\delta, \eta}$ be the subset of N_{δ} characterized by: $\mathbf{u} \in M_{\delta, \eta}$ if and only if

1. $u_0 < \widehat{u}_0^\varepsilon$,
2. $v_{2k+1}^4 < u_{2k+1} < 1 - \eta$ for $k \in \{2, 3, \dots, 1 + p - q\}$,
3. $(-1)^i u_i < (-1)^i u_i^\varepsilon$ for the remaining indices i .

Let $M_{\delta,\eta}^-$ denote the subset of $\partial M_{\delta,\eta}$ where the flow Ψ^t points out of $M_{\delta,\eta}$. A similar homotopy to the one in the proof of Lemma 5.5 furnishes that

$$H_*(M_{\delta,\eta}, M_{\delta,\eta}^-) \cong H_*(N_\delta, N_\delta^-) \cong H_*(\mathbf{H}(\mathbf{u} \# \mathbf{w}, \mathcal{E}; 2p)).$$

Theorem 7.3. *The index $H_*(h(\mathbf{u} \text{ rel } \mathbf{w}))$ is given by*

$$H_*(\mathbf{H}(\mathbf{u} \# \mathbf{w}, \mathcal{E}; 2p)) = \begin{cases} \mathbb{Z}, & \text{if } k = 2q - 1, \\ 0, & \text{otherwise.} \end{cases} \quad (7.2)$$

Proof. The set $N = \text{cl}[\mathbf{u}]_\varepsilon \text{ rel } \mathbf{w}$ is a $2p$ -dimensional set which is homotopic to the unit cube $[0, 1]^{2p}$, with $\mathbf{u} \in N$ if and only if

1. $u_0^1 \in [v_0^1, -1]$,
2. $u_{2i+1} \in \begin{cases} [-1, 1] & : \text{ if } 1 < i < 2 + p - q, \\ [+1, v_1^1] & : \text{ otherwise,} \end{cases}$
3. $u_{2i} \in \begin{cases} [-1, v_2^1] & : \text{ if } 1 < i < 3 + p - q, \\ [v_2^1, 1] & : \text{ otherwise.} \end{cases}$

If u_{2i+1} reaches the boundary and $i \in \{2, 3, \dots, 1 + p - q\}$ then the crossing number of the free strand \mathbf{u} with the skeleton \mathbf{w} increases. Likewise, if u_{2i} reaches the boundary for $i \in \{2, 3, \dots, 2 + p - q\}$ then the crossing number increases as well. On the other hand if some other anchor point reaches the boundary of its interval then the crossing number decreases. Hence N^- is the set on which some u_j , $j \notin \{4, 5, \dots, 4 + 2p - 2q\}$, attains the boundary. The pointed space $[N, N^-]$ is thus homotopic to $([0, 1]^{2q-1}, \partial[0, 1]^{2q-1})$. Hence $H_*(\mathbf{H}(\mathbf{u} \# \mathbf{w}, \mathcal{E}; 2p)) = H_*(N, N^-)$ is given by (7.2). ■

Non-triviality of the index $H_*(\mathbf{H}(\mathbf{u} \# \mathbf{w}, \mathcal{E}; 2p))$ stated in Theorem 7.3 concludes the second part of Theorem 1.8. A lower bound on the number of geometrically distinct solution is given by $\beta_{p,q} = 2^{q-5}$ by counting how many fingers can still be realized using the procedure from the previous section. Indeed, by (7.1) there are $q - 5$ positions for fingers, indexed in I , which yields the lower bound.

Finally, let us call the local maxima below $+1$ ‘‘dimples’’. In the above construction these have indices $i = 2j + 1$, with $j = 2, \dots, 2 + p - q$. Hence in this construction we first have dimples and then fingers. For large p (compared to q) there are also many other possible distributions of alternately dimples and fingers. This leads, via a completely analogous proof, to many more solutions, a line of thought that we do not pursue here.

8. Proofs of the main theorems. Theorem 1.6 and 1.8 were proved in Sections 5 and 7. The multiplicity of solutions of type $[\sigma_1^2 \sigma_2^{2p}, p]$ is established in Section 6. The ordering relation

$$[\sigma_1^2 \sigma_2^4, 2] \prec [\sigma_1^2 \sigma_2^{2q_1} \dots \sigma_1^2 \sigma_2^{2q_n}, p],$$

is established via the product relation in Theorem 1.5, which is proved as follows. We start with noting that elements in \mathcal{Z} can be represented as products of fundamental blocks $[\sigma, p] =$

$[\sigma_1^2 \sigma_2^{2q_i}, p_i]$, analogous to the decomposition in Section 6.2. The ordering relation $[\sigma_1^2 \sigma_2^4, 2] \prec [\sigma_1^2 \sigma_2^{2q_i}, p_i]$ is proved by constructing isolating neighborhoods N_I via associated relative braid classes. For a type $[\sigma, p] \cdot [\sigma', p']$ we can then use the product isolating neighborhoods, or relative braid class $N_I \times N'_I$. Non-triviality of the Conley indices of N_I and N'_I then implies non-triviality of the Conley index for $N_I \times N'_I$, proving Theorem 1.5.

The Theorems 1.7 and 1.9 now follow by applying the product property in Theorem 1.5.

REFERENCES

- [1] B. Buffoni, A. R. Champneys, and J. F. Toland. Bifurcation and coalescence of a plethora of homoclinic orbits for a Hamiltonian system. *J. Dynam. Differential Equations*, 8(2):221–279, 1996.
- [2] A. R. Champneys. Homoclinic orbits in reversible systems and their applications in mechanics, fluids and optics. *Phys. D*, 112(1-2):158–186, 1998.
- [3] C. Conley. *Isolated invariant sets and the Morse index*, volume 38 of *CBMS Regional Conference Series in Mathematics*. American Mathematical Society, Providence, R.I., 1978.
- [4] R. W. Ghrist, J. B. Van den Berg, and R. C. Vandervorst. Morse theory on spaces of braids and Lagrangian dynamics. *Invent. Math.*, 152(2):369–432, 2003.
- [5] A. Hatcher. *Algebraic topology*. Cambridge University Press, Cambridge, 2002.
- [6] W. D. Kalies, J. Kwapisz, J. B. Vandenberg, and R. C. A. M. VanderVorst. Homotopy classes for stable periodic and chaotic patterns in fourth-order Hamiltonian systems. *Comm. Math. Phys.*, 214(3):573–592, 2000.
- [7] L. A. Peletier and W. C. Troy. Multibump periodic travelling waves in suspension bridges. *Proc. Roy. Soc. Edinburgh Sect. A*, 128(3):631–659, 1998.
- [8] L. A. Peletier and W. C. Troy. *Spatial patterns*. Progress in Nonlinear Differential Equations and their Applications, 45. Birkhäuser Boston Inc., Boston, MA, 2001. Higher order models in physics and mechanics.
- [9] G. J. B. van den Berg, L. A. Peletier, and W. C. Troy. Global branches of multi-bump periodic solutions of the Swift-Hohenberg equation. *Arch. Ration. Mech. Anal.*, 158(2):91–153, 2001.
- [10] J. B. van den Berg. The phase-plane picture for a class of fourth-order conservative differential equations. *J. Differential Equations*, 161(1):110–153, 2000.
- [11] J. B. van den Berg, Lessard J.-P., and K. Mischaikow. Global smooth solution curves using rigorous branch following, 2010. To appear in *Mathematics of Computation*.
- [12] J. B. van den Berg, M. Kramar, and R. C. Vandervorst. Oscillatory solutions of fourth order conservative systems, 2010. Preprint.
- [13] J. B. van den Berg and J.-P. Lessard. Chaotic braided solutions via rigorous numerics: chaos in the Swift-Hohenberg equation. *SIAM J. Appl. Dyn. Syst.*, 7(3):988–1031, 2008.
- [14] J. B. van den Berg and R. C. Vandervorst. Second order Lagrangian twist systems: simple closed characteristics. *Trans. Amer. Math. Soc.*, 354(4):1393–1420 (electronic), 2002.